AN INVESTIGATION WITH FRACTAL GEOMETRY ANALYSIS OF TIME SERIES

A Thesis Submitted to
the Graduate School of Engineering and Sciences of
İzmir Institute of Technology
in Partial Fulfillment of the Requirements for the Degree of

MASTER OF SCIENCE

in Materials Science and Engineering

by
Aysun KAYA

July, 2005
İZMİR

We approve the thesis of **Aysun KAYA**

Date of Signature

.....
Asst. Prof. Serhan ÖZDEMİR **15 July 2005**
Supervisor
Department of Mechanical Engineering
İzmir Institute of Technology

.....
Assoc. Prof. Sedat AKKURT **15 July 2005**
Co-Supervisor
Department of Mechanical Engineering
İzmir Institute of Technology

.....
Prof. Dr. Halis PÜSKÜLCÜ **15 July 2005**
Department of Computer Engineering
İzmir Institute of Technology

.....
Prof. Dr. Refail ALİZADE **15 July 2005**
Department of Mathematics
İzmir Institute of Technology

.....
Asst. Prof. Gürsoy TURAN **15 July 2005**
Department of Civil Engineering
İzmir Institute of Technology

.....
Prof. Dr. Muhsin ÇİFTÇİOĞLU **15 July 2005**
Head of Department
İzmir Institute of Technology

.....
Assoc. Prof. Semahat ÖZDEMİR
Head of the Graduate School

BORDERLINE - A FRACTAL POEM

When tallying the interface?
And then to pocks on grains of sand,
Where lies the ocean, where the land?
With surf and turf along the beaches,
Each into the other reaches.

Sand and water melt into
A frothy fuzzy slurried stew,
With fractal sand grains swimming wild
And fractal drops on beaches piled.
And algae green, a form of life
Which further mediates the strife
Incorporates a snatch of each.
So much for life along the beach.

Now intertwining earth and air
Are ferns and bees and other fare.
And one more question if you'll hear it:
Are we flesh or are we spirit?
Does God exist and script the play
Or are we, rather, chunks of clay?
Lovers know as they entwine.
Life is just a borderline.

Ed Seykota, October 15, 1986

ABSTRACT

In this thesis, three kinds of fractal dimensions, correlation dimension, Hausdorff dimension and box-counting dimension were used to examine time series. To demonstrate the universality of the method, ECG (Electrocardiogram) time series were chosen. The ECG signals consisted of ECGs of three persons in four states for two applications. States are normal, walk, rapid walk and run. These three people are selected from the same age, and height group to minimize variations. First application was made for approximately 1000 samples of size of ECG signals and the second for the whole of the measured ECG signals. Fractal dimension measurements under different conditions were carried out to find out whether these dimensions could discriminate the states under question. A total of 24 ECG signals were measured to determine their corresponding fractal dimensions through the above-mentioned methods. It was expected that fractal dimension values would indicate the states related to the different activities of the persons. Results show that no direct link was found connecting a certain dimension to a certain activity in a consistent manner. Furthermore, no congruence was also found among the three dimensions that were employed. According to these results, it can be stated that fractal dimension values on their own may not be sufficient to identify distinct cases hidden in time series. Time series analysis may be facilitated when additional tools and methods are utilized as well as fractal dimensions at detecting telltale signs in signals of different states.

ÖZET

Bu tezde zaman serilerini incelemek için üç çeşit fraktal boyut, korelasyon boyutu, Hausdorff boyutu ve kutu sayma boyutu kullanılmıştır. Metodun evrenselliğini göstermek için EKG (Elektrokardiyogram) zaman serileri seçilmiştir. EKG sinyalleri dört durumda iki uygulama için üç kişinin EKG'lerinden oluşmaktadır. Durumlar normal, yürüme, hızlı yürüme ve koşmadır. Varyasyonları mümkün olduğu kadar azaltmak için bu üç kişi aynı yaş ve boy grubundan seçilmiştir. Birinci uygulama yaklaşık 1000 örnek büyüklüğündeki EKG sinyalleri için ve ikincisi EKG 'lerin tam ölçümleri için yapılmıştır. Değişik şartlar altında fraktal boyut ölçümleri bu boyutların sorgu altındaki durumları ayırt edip edemeyeceğini öğrenmek için tatbik edilmiştir. Toplam 24 EKG sinyali yukarıda değinilen metodlarla boyut karşılıklarını belirlemek için ölçülmüştür. Fraktal boyut değerlerinin, kişilerin farklı aktivitelere göre durumlarını işaret edeceği beklenmiştir. Sonuçlar belirli bir boyutun belirli aktiviteye tutarlı bir biçimde bağlantısı olmadığını göstermiştir. Dahası, kullanılan üç boyut arasında uygunluk bulunamamıştır. Bu sonuçlara göre fraktal boyut değerlerinin kendi başına zaman serilerinde saklı farklı durumları belirlemek için yeterli olmadığı ifade edilebilir. Zaman serileri analizleri fraktal boyutlar gibi, değişik durumların sinyallerinde farklılığı açığa vuran işaretlerin bulunmasında ek alet ve metodlar kullanılarak kolaylaştırılabilir.

TABLE OF CONTENTS

LIST OF FIGURES

Figure **Page**

LIST OF TABLES

CHAPTER 1

INTRODUCTION

Until recently, fractals have remained a novelty in explaining strange phenomena in nature. Today, it is realized that the capability of fractals is beyond the basic self-similar illustration of snow flakes. The use of fractals is in the range from interpolation, estimation, even as far away as to data compression and modelling. Detection of faults in mechanical systems has come under spotlight increasingly ever so with the advent of intelligent modelling tools in this field. By the use of fractals, the analysis of time series could point at inherent flaws, cracks, and impurities in the material.

This thesis presents a tentative approach to time series analysis which is based on the geometry of fractals. Chaotic systems, which seem to be a distant topic, exhibit rich and surprising mathematical structures. In this context, deterministic chaos provides a striking interpretation for irregular temporal behaviour and anomalies in systems which do not seem to be inherently stochastic. The most direct link between chaos theory and the real world is the analysis of time series of real systems in terms of nonlinear dynamics. Sometimes time series are so complex that they could not be examined by traditional methods. Problems of this kind are typical in biology, physiology, geophysics, economics, to name a few, as well as engineering and many other sciences.

This thesis is based on a mathematical technique to illustrate the analysis of ECG signals. ECG signals were chosen for applications in order to show that this approach is universal. The ECG is a representative signal containing information about the condition of the heart. The shape and size of the P-QRS-T wave, the time intervals between its various peaks, etc. may contain useful information about the nature of disease afflicting the heart.

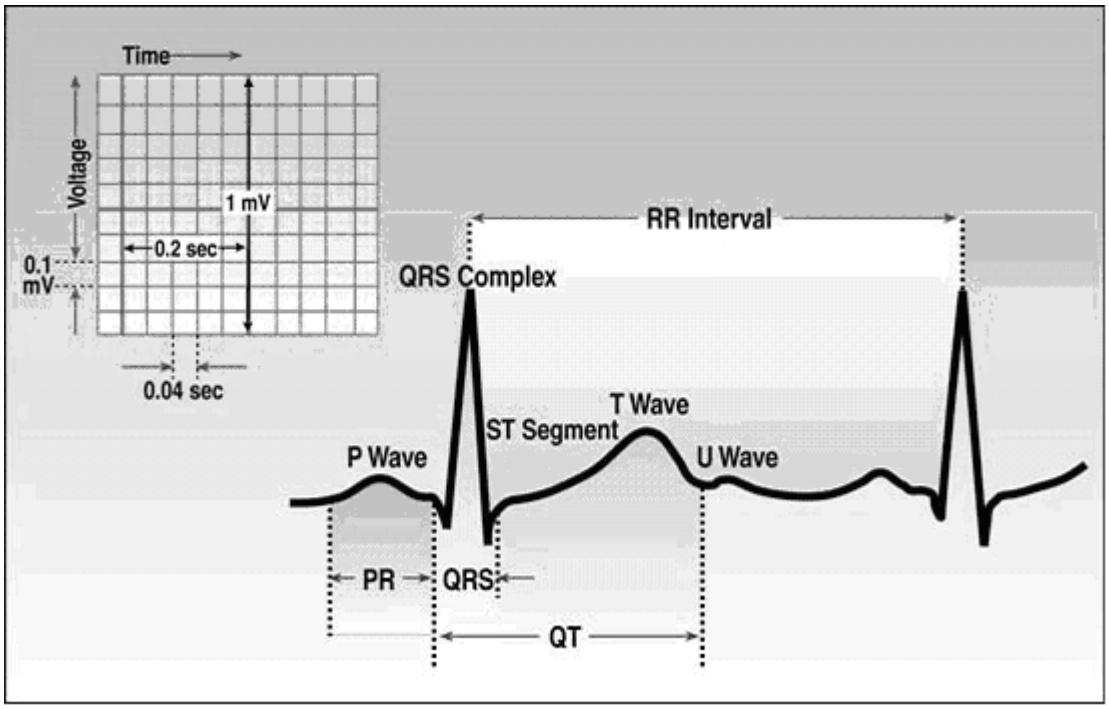

Figure 1.1. The shape and size of the P-QRS-T wave of the electrocardiogram (ECG)

Figure 1.1. defines the shape and size of the P-QRS-T wave of the electrocardiogram, this is essential for cardiologists to determine the classification of heart failure from ECG, "(Dublin 2000)". The characteristics of all interval (PR, QRS, QT, RR) on Figure 1.1. can change by specific heart failures. Sinus Arrhythmia is considered as normal, where other sinus Arrhythmia shapes or intervals could lead us to heart disease e.g. atrial Fibrillation, wandering pacemaker, multifocal atrial tachycardia. ECG signals are widely examined signals, thinking the significance in humans' life. On the other hand decisions about ECG signals were made through doctors and expert technicians, handling the intervals between P-QRS-T waves. In this thesis these observations are wanted to be demonstrated in numerical results, using three kinds of fractal dimension methods in fractal geometry.

Classical geometry makes arrangements for an initial approach to the physical objects structure. It is a way of communication for designs of technological products and natural creations. Fractal geometry can be described as a branch of classical geometry, with some differences in dimension property.

Fractal geometry is also the premier level for computation of rational roughness, in other words, the first scientific stage of researching the smoothness. Roughness is

present everywhere in nature. This reason is adequate to prove variety of the usage of fractals.

The history of fractals has begun by the research of Gaston Julia, and continued with findings of Benoit Mandelbrot. Benoit Mandelbrot was one of the first to discover fractals. Mandelbrot extracted the “fractal” term from “frangere”, a Latin verb, meaning to break or fragment. He was examining the shapes created by Gaston Julia, by iterating a simple equation and mapping this equation in the complex plane, where Gaston Julia, a mathematician in the 1920’s (who was working without the benefit of computers) could not describe these shapes using Euclidean geometry, “(Barnsley 1993)”.

From a mathematical aspect, fractals are embodiments of iterations of nonlinear equations, commonly building a feedback loop. By creating a vast number of points using computers these wonderfully complex images, called fractals, were discovered. This set of points is produced, by using the output value of the previous calculation as the input value of the current calculation. Two important properties of fractals could be arranged as:

- Fractional dimensions
- Self-similarity

Self-similarity means that the fractal image, at every level reiterates itself. For example, Sierpinski’s Triangle is a triangle within ever smaller triangles, on and on. A lot of natural shapes exhibit the self-similarity characteristic. Almost all objects possess this feature. Fractional dimension signifies that a shape is neither 1, 2 or 3 dimensional, practically may fall between integer numbers, resulting from fractions. Mandelbrot set a theory that fractals have a fractional dimension between 1 and 2, whereas in Euclidean geometry, image dimension is always given in integer units.

By studying fractals, a whole new geometry has been created by mathematicians depicting the universe, beyond the boundaries of Euclidean geometry. Traditional Euclidean models come into view, simpler as they are magnified, the shape looks more and more like a straight line. But very little in nature is so regular. The need to deduce irregular shapes using geometry, namely fractal geometry, could provide to express the complexities of these shapes.

Fractals can be thought of a mirror, describing these irregular shapes. They represent the relationships between disparate parts of the universe in a visual manner,

demonstrating the interdependence of all things in nature. They allow us to view the complexity of chaos and order. Fractal is a mathematical set with a high degree of geometrical complexity, which can model many classes of time series data as well as images.

With fractals, scientists gained the knowledge that the scale did not change the outline of the original shape. It can reiterate itself regardless of size and therefore it takes a new understanding for scaling and measuring. Before fractal geometry, calculus helped to find the area or the perimeter of irregular shapes by creating rectangles of smaller dimensions, but this is also a limit to escape from simple models.

Fractals are interesting, as more detail shows up indefinitely as one gets closer. A fractal dimension depends on how much space the object takes up as it twists. As a fractal fills a plane progressively more, its dimension approaches two. So a fractal landscape made up of a large hill covered with tiny bumps would be close to dimension two, while a rough surface composed of many medium sized hills would be close to dimension three, "(Web_1 1998)". It also could be said, because of wonderful shapes, fractals are the place, where math and art come together.

As it is mentioned above, fractal dimension is one of the important features of fractals, because it contains information about their geometrical structure. A more clear definition, fractal dimension is one measure, which is useful for comparing two fractal images. Fractal geometry provides a means to get rid of the restriction on dimension by R-dimensional measurement features, where R can be any fractional (Real) number and so the fractional dimensions coined the "fractal geometry" term. On the other hand not all images are true fractals. Any set of discrete data points, no matter how fine the spacing between points, is not truly fractal because you can "zoom-in" such that all you see is an individual point or the blank space between points, "(Butterfield 1991)".

The inspiration behind using fractal transformations is to develop a novel high - speed feature extraction technique. Also in the area of pattern recognition and image processing, the fractal dimension has been used for image compression, texture segmentation and feature extraction. One of the basic characteristics of a fractal is its dimension, as it is seen. The main idea is to describe the complexity of the image through a new parameter. Fractal dimension can be thought as the basic parameter of a fractal set, which represents much information related to signal's geometric features.

Mathematically, a fractal dimension is a fraction greater than the topological dimension of a set and remains constant whatever the scale. The more the fractal

dimension is close to the topological dimension, the more the fractal surface looks smooth, "(Tang et al. 2002)".

On the other hand it should be noted that the modelling of signals through fractal geometry could be used in fault diagnosis analysis. Various theoretical properties of the fractal dimension, including some explicit formulas, are developed to be successful in order to detect faults in a system.

Some definitions and properties on fractals might further be expounded. For example, the term, "Gaussian fractal", denotes any geometric fractal shape generated by a Gaussian random process. It is a form of fractional Brownian cluster, fractal sets are related to the fractional Brownian motions, FBM, denoted by $B_H(t)$, where the exponent, an essential exponent denoted by H is deeply rooted in two fields of knowledge that were thoroughly removed from each other until fractal geometry spanned the abyss between them, H was defined by the hydrologist H.E. Hurst . H should satisfy $0 < H < 1$. In the key case $H = ½$, FBM reduces to WBM, "(Leung and Romagnoli 2000)".

The prototype Gaussian fractals are generated by the original Brownian motion, for which Wiener provided the mathematical theory. The requirement for constructions beyond WBM appeared independently in finance and physics. In the natural harsh phenomena that should be inspected, the pathology of nature is not uncontrollable, because it complies a form of invariance or symmetry that overlaps nature and mathematics, and is called scale invariance, or scaling.

The more specific term self-affinity, expresses invariance under some linear reductions and dilations, which ordinarily implies uniformly global statistical dependence. Self-affinity takes at least three distinct forms: unifractality, mesofractality, multifractality. The far better known notion of self-similarity is the special case corresponding to isotropic reductions. Here, the lake and island coastlines are the best example to define self-similarity, while the relief itself is self-affine. That is the Gaussian records that represent reliefs are invariant under linear contractions whose ratios are different along the axes of the free variables and the axis of the function, "(Wu et al. 2004)". Especially, the concept of fractal dimension experiences a very extensive general statement and becomes less directly convincing than in self-similar contexts. Roughness is the form of wildness of self-affinity.

In this chapter, fractals and fractal geometry are mentioned roughly, detailed explanations will be made in the following chapters.

Chapter 2 introduces the basic topological ideas that are needed to describe subsets to spaces such as R^2 which provide a suitable setting for fractal geometry. The concepts introduced include openness, closeness, compactness, convergence, completeness, connectedness and equivalence of metric spaces. This chapter includes also the concept of fractal dimension and other definitions. The fractal dimension of a set is a number that tells how densely the set occupies the metric spaces in which it lies. It is invariant under various stretching and squeezing of the underlying space. This makes the fractal dimension meaningful as an experimental observation; it possesses certain robustness and is independent of the measurement units.

Chapter 3 deals with combining ECG signals with fractal geometry. The aim of this chapter is to show the usage of fractals in the field ECG signals. It will be explained through specified box-counting method, which has been mentioned in chapter 2. In addition, the software packages, which are used in experiments, will be introduced.

Chapter 4 is concerned with examples, how to make the calculation of ECG signals parameters. It will be shown with diagrams, graphs and some visualizations. The necessary information about ECG signals will be also given.

Chapter 5 will construct the discussion and the conclusion parts of this thesis.

CHAPTER 2

FRACTALS AND FRACTAL GEOMETRY

The balance between the roles of geometry and analysis is very distinctive in the field of sciences. A combination of analysis and geometry should be found in order to expand the aspect in science. Before fractal geometry, any measure of roughness quantity was not agreed-upon. The significant point in this thesis is to apply the scale–invariance property to ECG time series. Approximately expressed, fractal geometry is the study of scale–invariant roughness.

Fractal geometry claims that roughness cannot be measured by any quantitiy taken from other examinations. In the way of fractality being scale- invariance, roughness can be measured most naturally by the parameters.

2.1. Why Fractals?

Fractals, as these shapes are called, also must be without translational symmetry that is, the smoothness connected to Euclidean lines, planes, and spheres. Instead of a rough, jagged quality is kept in existence at every scale at which an object can be tested. Fractals are not referred solely to the region of mathematics. If the interpretation is made a bit wider, such objects can be established in essence everywhere in nature.

The distinction is that "natural" fractals are randomly, statistically, or stochastically rather than exactly scale symmetric. The harsh shape exibited at one length scale bears only a near similarity to that at another, but the length scale being used is not obvious just by watching the shape. Moreover, there are both upper and lower limits to the size range over which the fractals in nature are surely fractal.

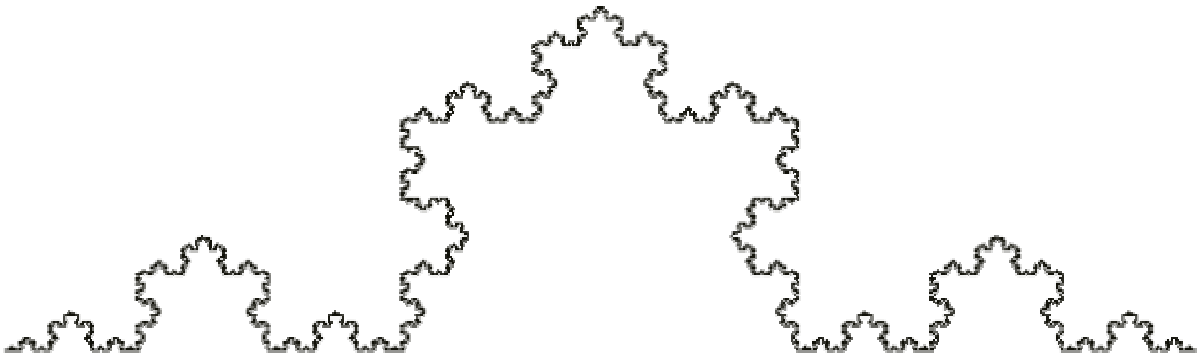

Figure 2.1. The Koch Curve

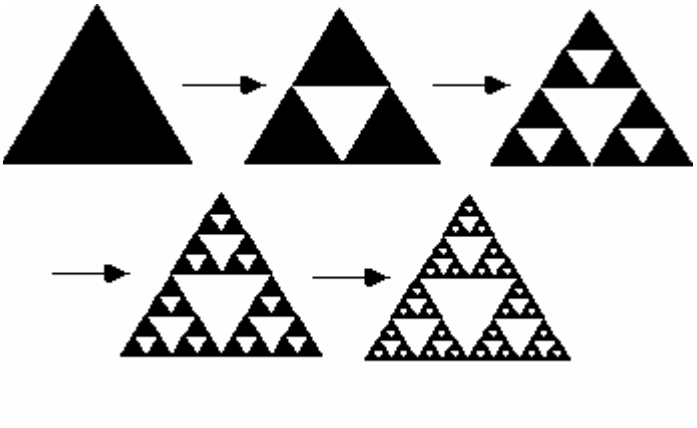

Figure 2.2. Sierpinski Triangle

Famous examples are the Koch curve and Sierpinski triangle, which can be seen in Figure 2.1. and Figure 2.2. Fractals may not actually give us a better way to measure coastlines, but they do help us see patterns in real objects and systems that appear not to be patterned, "(Web_1 1998)". Fractal dimensions put to practical use the jagged edges of clouds, mountain and coastlines. They also deal with the loopy chaotic motions of weather, the economy, brain signals and heartbeats.

2.2. Scale-Invariance and Fractal Relation

The question to explain why so many natural objects are scale-invariant, is very important. This theme concerns both physics and astronomy, and also synthetic structures, as examples, finance and computers. While "mathematical proof" is a nicely-specified concept where, "physical explanation" is a tricky fundamental idea. But computer simulation and fractals each conclued a significant wrinkle.

Attractors and repellers of dynamical systems; fractality in phase space is fully explained by chaotic dynamics. In many scientists' minds, explanation is the best implemented in terms of a dynamic process that transforms an arbitrary initial condition into what is observed and must be explained, "(Barnsley and Demko 1985)".

Fractals, which are consequential physical objects in real space, go into the problems that are governed by partial differential equations PDEs, "(Barnsley 1986)". Last mentioned, a center topic in both sciences, mathematics and physics, have succeeded against many unknowns of nature and guard an eternal inherent beauty. It is the fact that physics is described by equations such as those of Laplace, Poisson, and Navier-Stokes. An important degree of local smoothness is provided by differential equations, although adjacent test shows isolated singularities or catastrophes. Inversely, fractality results from everywhere dense roughness and fragmentation. This is the best evidence, why fractal models in varied fields were initially noticed as being "anamolies" that stand in direct opposition with one of the most stable establishings of science. Many concrete situations where fractals are observed involve equations having free and moving boundaries and interfaces, and singularities are not prescribed in the statement of a problem, but determined by the problem's solution, "(Curry et al. 1983)". Under broad conditions, which largely remain to be specified, show us these free boundaries, interfaces and singularities converge to suitable fractals.

A sort of clusters comprise a third class of very influential fractals that elevate problems for mathematics and physics and are presently experiencing quick progress. Therefore, in the situation of the physical clusters conversed previously, fractality is the geometric complement of scaling and renormalization, that is why the analytic poperties of those objects pursue the power law relations. Some issues concerning mathematics, remain open, but the overall renormalization structure is strongly fixed.

This chapter introduces, as it is mentioned earlier, also the basic topological ideas that are needed to describe subsets to spaces such as R^2. They provide a suitable setting for fractal geometry. The concepts introduced include openness, closedness, compactness, convergence, completeness, connectedness and equivalence of metric spaces. It includes also the concept of fractal dimension and other important definitions (Detailed fractal geometry definitions could be found in Appendix A).

2.3. Fractal Dimensions and Their Dimension Properties

Whether natural or synthetic, all fractals have special fractal dimensions. The fractal dimension, with the symbol D, a chracteristic of fractals, shows clearly unlike other criteria to be an invariant measure of the roughness of the fractures in materials. It has a sence that the words fracture and fractal came from the same root, fract.

Seen that there are some differences, these are not the same as the familiar Euclidean dimensions, quantified in discrete whole integers 1, 2, or 3. A fractal dimension implies the scope to which the fractal object fills the Euclidean dimension in which it is embedded and it is usually noninteger. In other words, finding fractal dimension is a search for an underlying order in things that appear randomly for patterns. Most real objects having serrated edges and are irregular they can not exactly fit simple classification in integer dimensions. For instance, the dimension of the edge of a coastline appear to be one, it's just a wiggly line. On the other hand, it is so twisted that it fills more of a two-dimensional rectangle than a straight line or even a smooth curve. Through this way the fractal dimension, a measure of irregularity degree allows to give us finally feasible knowledge. A system can be revealed as chaotic even though it appers to be random by measuring the fractal dimension of its phase space graph or attractor. Measurement of fractal dimensions from snapshots of chaotic dynamical systems supplies some intuitions into the dynamic forces which control them.

2.3.1. Hausdorff Measure and Dimension

Hausdorff dimension has the advantage of being defined for any set, and is mathematically convenient, as it is based on measures, which are relatively easy to manipulate. A major disadvantage is that in many cases, it is hard to calculate or to estimate by computational means. D can take on noninteger values, is based on metric properties, and gives the right values for the sets for which it can be computed. Lurking behind, were nondifferentiable and infinitely discontinuous functions, singular monotone-increasing functions, the Hausdorff dimension D, and the Hölder exponent.

U : Non-empty subset of n-dimensional Euclidean space, IR^n .

Diameter of U : $|U| = \sup\{|x-y| : x,y \in U\}$, i.e. the greatest distance apart of any pair of points in U.

$\{U_i\}$: Countable (finite) collection of sets of diameter at most δ that cover F, i.e.

$F \subset \bigcup_{i=1}^{\infty} U_i$ with $0 < |U_i| \leq \delta$ for each I .(I : interval)

Then we say $\{U_i\}$ is a δ- cover of F. (A collection of sets with maximum diameter δ that covers F).

$$H_{\delta}^{s}(F) = \inf\left\{ \sum_{i=1}^{\infty} |U_i|^s : \{U_i\} \right\} \quad \text{is a } \delta\text{- cover of F} \qquad (2.1)$$

Where F is a subset of IR^n, s is a non-negative number. Thus we look at all covers of F by sets of diameter at most δ and seek to minimize the sum of the s^{th} powers of the diameters, as it is seen in Figure 2.3.

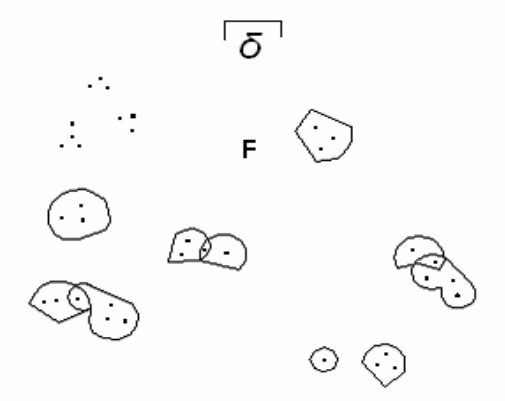

Figure 2.3. A set F and two possible δ- covers for F.

The infimum of $\sum | U_i |^s$ over all such δ-covers $\{U_i\}$ gives $H^s_\delta(F)$. As δ decreases, the class of permissible covers of F is reduced. Therefore, the infimum $H^s_\delta(F)$ increases, and approaches a limit as $\delta \to 0$.

$$H^s(F) = \lim_{\delta \to o} H^s_\delta(F) \qquad (2.2)$$

$H^s(F)$ is called the s- dimensional Hausdorff measure of F.

2.3.1.1. Characteristics of Hausdorff Measure

- $H^s(\emptyset) = 0$
- $H^s(E) \leq H^s(F)$, E is contained in F
- $H^s(\bigcup_{i=1}^{\infty} F_i) = \sum_{i=1}^{\infty} H^s(F_i)$, if $\{F_i\}$ is any countable collection of disjoint Borel sets.
- $H^n(F) = C_n \, vol^n(F)$, i.e. for subsets of IR^n, n-dimensional Hausdorff measure is, to within a constant multiple, just n-dimensional Lebesgue measure, namely the usual n-dimensional volume.

$H^0(F)$: number of points in F.

$H^1(F)$: the lenght of a smooth curve, F.

$H^2(F)$: $(4/\pi) \times$ area (F) , F being a smooth surface.

$H^3(F)$: $(6/\pi) \times$ vol (F)

$H^m(F)$: $C_m \times \text{vol}^m(F)$ if F is a smooth m-dimensional submanifold of IR^n (i.e. m-dim surface)

2.3.1.2. Properties of Hausdorff Measure

Open Sets : If $F \subset IR^n$ is open, then $\dim_H F = n$. Since F contains a ball of positive n-dimensional volume.

Smooth Sets : If F is a smooth (i.e. continuously differentiable) m- dimensional submanifold (i.e. m- dimensional surface) of IR^n then $\dim_H F = m$.

In particular, smooth curves have dimension 1 and smooth surfaces have dimension 2.

Monotonicity : If $E \subset F$ then $\dim_H E \leq \dim_H F$.

This is immediate from the measure property that $H^S(E) \leq H^S(F)$ for each s.

Countable Stability : If F_1, F_2 ... is a countable sequence of sets then

$\dim_H \bigcup_{i=1}^{\infty} F_i = \sup_{1 \leq i \leq \infty} \{ \dim_H F \}$.

Certainly, $\dim_H \bigcup_{i=1}^{\infty} F_i \geq \dim_H F_j$ for each j from the monotonicity property. On the other hand, if $s > \dim_H F_i$ for all i , then $H^S(F_i) = 0$ so that $H^S(\bigcup_{i=1}^{\infty} F_i) = 0$, giving the opposite inequality.

Countable Sets : If F is countable then $\dim_H F = 0$. For if F_i is a single point, $H^0(F_i) = 1$ and $\dim_H F_i = 0$ so by countable stability $\dim_H \bigcup_{i=1}^{\infty} F_i = 0$.

Proposition (2)

Let $F \subset IR^n$ and suppose that $f : F \rightarrow IR^m$ satisfies a Hölder condition

$| f(x) - f(y) | \leq c | x - y |^{\alpha}$, $x,y \in F$

Then $\dim_H f(F) \leq (1/\alpha)\dim_H F$

Corollary

If $f : F \rightarrow IR^m$ is a bi-Lipschitz transformation, then $\dim_H f(F) = \dim_H F$

This corollary reveals a fundamental property of Hausdorff dimension: Hausdorff dimension is invariant under bi- Lipschitz transformations.

Which is remiscent to if the topological invariants of two sets differ then there can not be a homeomorphism (continuous one–to–one mapping with continuous inverse) between the two sets.

In topology, two sets are regarded as the same if there is a homeomorphism between them. One approach to fractal geometry is to regard two sets as the same if there is a bi- Lipschitz mapping in between.

Proposition :

A set $F \subset IR^n$ with $\dim_H F<1$ is totally disconnected .

Net Measures :

For the sake of simplicity ; let F be a subset of the interval [0,1). A binary interval is an interval of the form $[r2^{-k}, (r+1)2^{-k}]$

where $k = 0,1,2...$; $r = 0,1..., 2^k -1$.

$M^S_\delta(F) = \inf\{\sum | U_i |^S : \{ U_i \}$ is a δ-cover of F by binary intervals $\}$

$M^S(F) = \lim_{\delta \rightarrow 0} M^S_\delta(F)$ (Net Measures)

$H^S(F) \leq M^S(F) \leq 2^{S+1} H^S(F)$

It follows that the value of s at which $M^S(F)$ jumps from ∞ to 0 equalls the Hausdorff dimension of F, i.e. both definitions of measure give the same dimension.

For certain purposes, net measures are much more convenient than Hausdorff measures. This is because two binary intervals are either disjoint or one of them is contained in the other, allowing any cover of binary intervals to be reduced to a cover of disjoint binary intervals.

2.3.1.3. Scaling Property

$$H^s(\lambda F) = \lambda^s H^s(F) \tag{2.3}$$

where $\lambda F = \{\lambda x : x \in F\}$, i.e. the set F is scaled by factor λ .

Proposition (1)

Let $F \subset IR^n$ and $f : F \rightarrow IR^m$ be a mapping such that

$| f(x) - f(y) | \leq c | x - y |^{\alpha}$, $x,y \in F$ for constants $c>0$ and $\alpha >0$. Then for each s :

$$H^{s/\alpha}(f(F)) \leq C^{s/\alpha} H^s(F) \tag{2.4}$$

Case

$\alpha = 1$ gives Lipschitz mapping

else, Hölder condition of exponent α.. Any differentiable function with bounded derivative is necessarily Lipschitz as a consequence of the mean value theorem. If f is an isometry, i.e.

$| f(x) - f(y) | = | x - y |$, then $H^s(f(F)) = H^s(F)$.

Hausdorff measures are translation and rotation invariant.

$H^s(F + z) = H^s(F)$, where $F + z = \{x + z : x \in F\}$.

2.3.1.4. Hausdorff Dimension

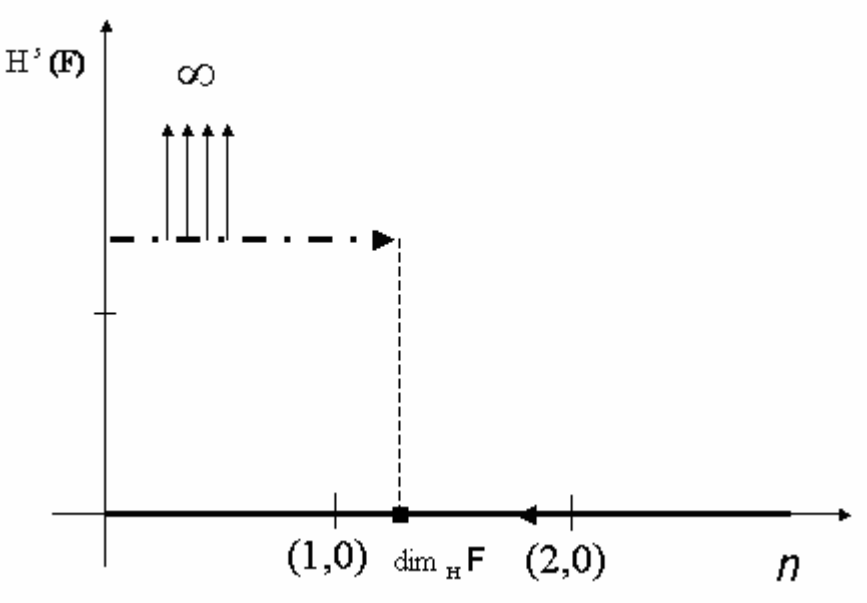

Figure 2.4. Medida Hausdorff Dimension Graph

$$\dim_H F = \inf\{s: H^S(F) = 0\} = \sup\{s: H^S(F) = \infty\} \qquad (2.5)$$

$$H^S(F) = \begin{cases} \infty \ , \ \text{if} \quad s < \dim_H F \\ \\ 0 \ , \ \text{if} \quad s > \dim_H F \end{cases}$$

Think of s as a variable between $0 \le s \le n$, it was shown in Figure 2.4. For a very simple example, let F be a flat disc of unit radius in IR^3. From familiar properties of length, area and volume,

$H^1(F) = \text{length}(F)\ \infty$;

$0 < H^2(F) = (4/\pi) \times \text{area}(F) < \infty$;

$H^3(F) = (6/\pi) \times \text{vol}(F) = 0$.

Thus $\dim_H F = 2$ with $H^S(F) = \infty$ if $s < 2$

$H^S(F) = 0$ if $s > 2$

2.3.1.5. Alternative Definitions of Dimension

Fundamental to most definitions of dimension is the idea of measurement at scale δ, we measure a set in a way that ignores irrregularities of size less then δ, and see how these measurements behave as $\delta \to 0$.

Our measurement, $M_\delta(F)$ might be the number of steps required by a pair of dividers set at length δ to traverse F. A dimension of F is then determined by the power low (if any) obeyed by $M_\delta(F)$ as $\delta \to 0$. (See Figure 2.5)

If $M_\delta(F) \sim c\delta^{-S}$, c and s being constants, we may say that F has dimension s with c regarded as the s-dimensional length of F.

Taking logarithims,

$\log M_\delta(F) \cong \log c - s \log \delta$

$$s = \lim_{\delta \to 0} \frac{\log M_\delta(F)}{-\log \delta} \tag{2.6}$$

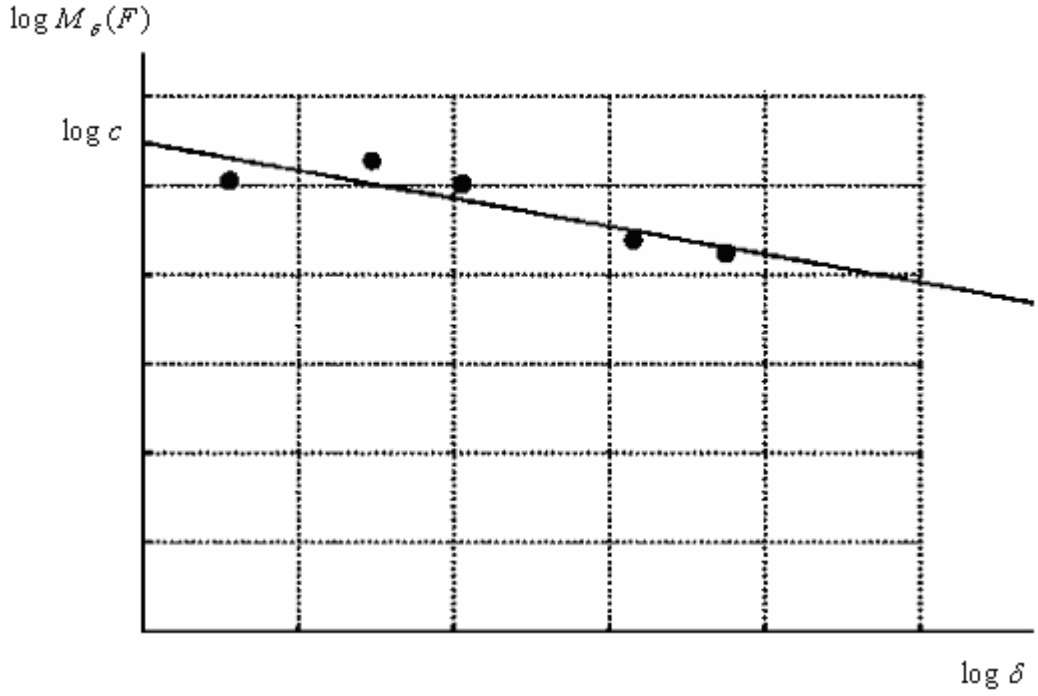

Figure 2.5. Power Law Assumption $M_\delta(F) \sim c\delta^{-S}$

There are no hard and fast rules for deciding whether a quantity may reasonable be regarded as a dimension. In general, one looks for some sort of scaling behaviour, a naturalness of the definition in the particular context and properties typical of dimensions such as:

Monotonicity : If $E \subset F$ then $\dim_H E \leq \dim_H F$.

Stability : $\dim_H (E \cup F) = \max (\dim_H E , \dim_H F)$.

Countable Stability : $\dim_H \bigcup_{i=1}^{\infty} F_i = \sup_{1 \leq i \leq \infty} \{ \dim_H F \}$.

(Of the union of finite sets, the dimension of the union is the supremum of the set within the union).

Geometric Invariance : $\dim_H f(F) = \dim_H F$ if F is a transformation of IR^n such as a translation , rotation, similarity or affinity.

Lipschitz Invariance : $\dim_H f(F) = \dim_H F$ if F is a bi- Lipschitz transformation.

(Before and after the transformation, dimension stays the same).

Countable Sets : $\dim_H F = 0$ if F is finite or countable.

Open Sets : If F is an open subset of IR^n, then $\dim_H F = n$.

Smooth Manifolds : $\dim_H F = m$ if F is a smooth m- dimensional manifold .

Caution :

Diffrent definitions of dimension could produce different results.

Note : All the usual dimensions are Lipschitz invariant, and therefore, geometrically invariant.

The Hausdorff dimension is essential to define for arbitrary subsets of metric scales by a process involving an infimum and supremum. On the other hand it is very difficult to calculate this almost wonderful fractal dimension. Therefore there is a need of using another fractal dimension. The box-counting dimension is one of the dimensions, which seems to be easy to calculate. This dimension will be used in this thesis and detailed application will be given in chapter 3.

2.3.1.6. Box-Counting Dimension

Box-counting dimension is also known as Kolmogorov entropy, entropy dimension, capacity dimension, logarithmic density and information dimension.

Definition :

F : Non- empty bounded subset of IR^n.

$\mathbf{N}_\delta$**(F)** : The smallest number of sets of diameter at most δ which can cover F. The lower and upper box-counting dimensions of F are:

$$\underline{\dim}_B(F) = \underline{\lim}_{\delta \to 0} \frac{\log N_\delta(F)}{-\log \delta} \tag{2.7}$$

$$\overline{\dim}_B(F) = \overline{\lim}_{\delta \to 0} \frac{\log N_\delta(F)}{-\log \delta} \tag{2.8}$$

If these are equal, we refer to the common value as the box-counting dimension, or box-dimension of F.

$$\dim_B(F) = \lim_{\delta \to 0} \frac{\log N_\delta(F)}{-\log \delta} \tag{2.9}$$

$\mathrm{N}_\delta(\mathrm{F})$ is any of the following:

i. The smallest number of closed balls of radius δ that cover F.
ii. The smallest number of cubes of side δ that cover F.
iii. The number of δ-mesh cubes that intersect F.
iv. The smallest number of sets of diameter at most δ that cover F.
v. The largest number of disjoint balls of radius δ with centers in F.

2.3.1.7. Minkowski Content

Recall δ-parallel body F_δ of F

$F_\delta = \{x \in IR^n : \left| x - y \right| \leq \delta \text{ for some } y \in F\}$

We know consider the rate at which the n-dimensional volume of F_δ shrinks as $\delta \to 0$. In IR^3, if F is a single point then F_δ is a ball of $vol(F_\delta) = 4/3\pi\,\delta^3$, if F is a segment of length "l" then F_δ is a sausage-like with $vol(F_\delta) \sim \pi l\,\delta^2$. If F is a flat set of area a then F_δ is a thickening of F with $vol(F_\delta) \sim 2a\delta$. In each case $vol(F_\delta) \sim c\delta^{3-S}$ where the integer s is the dimension of F, so that exponent of δ is indicative of the dimension. The coefficient c of δ^{3-S} is known as the Minkowski Content of F, which is a measure of length , area or volume of the set as appropriate. If F is a subset of IR^n, and for some s $vol^n(F_\delta)/\delta^{n-S}$ tends to a positive finite limit as $\delta \to 0$, then it makes sense to regard F as s dimensional.

For example, for the case F being a point and F_δ a ball then

$3 = 3 - s \quad \Rightarrow \quad s = 0$ $\qquad\qquad$ $\delta^{\overbrace{3-S}^{\uparrow}}$ $\downarrow$ $4/3\pi\,\delta^3$

Note :

Box dimension is sometimes referred to as Minkowski dimension.

2.3.1.8. Properties of Box-Counting Dimension

i. A smooth m-dimensional submanifold of IR^n has $\dim_B F = m$

ii. $\underline{\dim}_B$ and $\overline{\dim}_B$ are monotonic

iii. $\overline{\dim}_B$ is finitely stable , i.e. $\overline{\dim}_B(E \cup F) = \max\{\overline{\dim}_B E\ ,\ \overline{\dim}_B F\}$ though $\underline{\dim}_B$ is not .

iv. $\underline{\dim}_B$ and $\overline{\dim}_B$ are Lipschitz invariant .Box dimensions behave just like Hausdorff dimensions under bi- Lipschitz and Hölder transformations .

Problems :

Let $\overline{F}$ denote the closure of F (i.e. the smallest closed subset of IR^n containing F)

$\underline{\dim}_B \overline{F} = \underline{\dim}_B F$

$\overline{\dim}_B \overline{F} = \overline{\dim}_B F$.

Consequence :

If F is a dense subset of an open region of IR^n then $\underline{\dim}_B F = \overline{\dim}_B F = n$

For example, Let F be the (countable) set of rational numbers between 0 and 1. Then $\overline{F}$ is the entire interval [0,1], so that $\underline{\dim}_B F = \overline{\dim}_B F = 1$

Thus countable sets can have non-zero box dimension. Moreover, the box-counting dimension of each rational number regarded as a one point set is clearly zero, but the countable union of these singleton sets has dimension 1. Consequently, it is genarally not true that

$$\dim_B \bigcup_{i=1}^{\infty} F_i = \sup_i \dim_B F_i \qquad (2.10)$$

This severely limits the usefulness of box-dimension. Small (countable) set of points can wreak havoc with the dimension.

Fractal dimensions conserve the knowledge display in the preasymptotics. It is an unavoidable expansion of quantitative measurement concerning “degree of raughness” and “degree of emptiness”. Moving beyond pure mathematics, the use of fractal dimension soon faced its own fresh “anomalies”.

From this point, a particular analysis exhibited many arguments involving the concept of dimension can be rephrased to be very attentive to the important information demonstrate in the preasymptotics but ruined by asymptotics. It can be shown especially the case for the heuristics to clarify negative dimensions. When it is positive, it is ordinary measure of degree of roughness. When it is negative, it presents an

interesting innovation, in other words, a numerical measure of the "degree of emptiness". It will be proper to give examples in order to explain this situation. In the plane, the intersection of line and point, or of two points, are said to be, respectively, of dimensionas -1 and -2. Surprising but true, such negative values can actually be obtained experimentally, "(Gilbert 1982)".

2.3.1.9. Relation to Hausdorff Dimension

$$H_{\delta}^{S}(F) \leq N_{\delta}(F)\, \delta^{S} \tag{2.11}$$

$$1 < H^{S}(F) = \lim_{\delta \to 0} H_{\delta}^{S}(F) \tag{2.12}$$

$\log N_{\delta}(F) + s \log \delta > 0$, if δ is sufficiently small. Thus;

$$s \leq \underline{\lim}_{\delta \to 0} \frac{\log N_{\delta}(F)}{-\log \delta} \tag{2.13}$$

so $$\dim_{H} F \leq \underline{\dim}_{B} F \leq \overline{\dim}_{B} F \tag{2.14}$$

Interpretations :

$$\dim_{B}(F) = \lim_{\delta \to 0} \frac{\log N_{\delta}(F)}{-\log \delta} \tag{2.15}$$

means $N_{\delta}(F) \sim \delta^{-S}$ for small δ, where $s = \dim_{B} F$. Or better put,

$$N_{\delta}(F)\, \delta^{S} \to \infty \quad \text{if} \quad s < \dim_{B} F \quad \text{and,} \tag{2.16}$$

$$N_{\delta}(F)\, \delta^{S} \to 0 \quad \text{if} \quad s > \dim_{B} F. \tag{2.17}$$

$$N_{\delta}(F)\, \delta^{S} = \inf \left\{ \sum_{i} \delta^{S} : \{U_i\} \text{ is a (finite) } \delta\text{- cover of } F \right\} \tag{2.18}$$

Note :

Box dimensions may be thought of as indicating the efficiency with which a set may be covered by small sets of equal size, whereas Hausdorff dimension involves coverings by sets of small but perhaps widely varying size.

Example :

Let F be the middle third Cantor set :

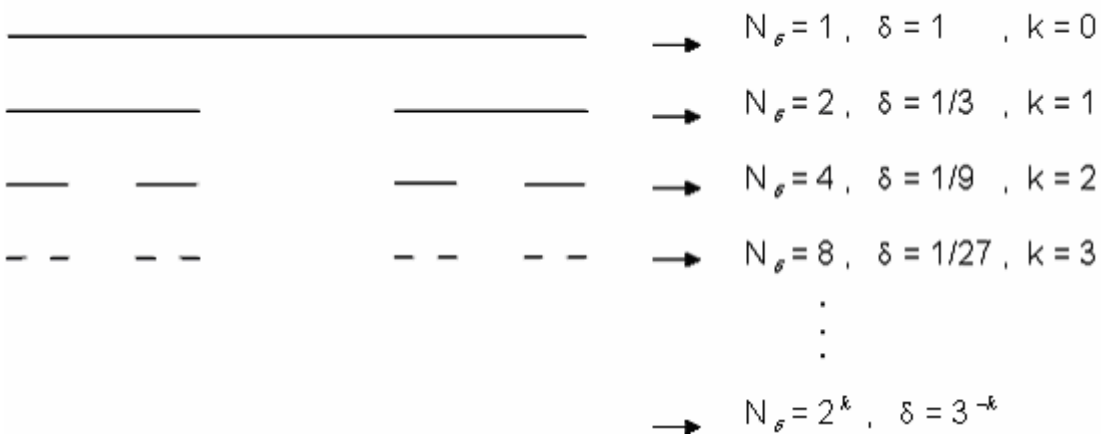

Figure 2.6. The Middle Third Cantor Set

$\underline{\dim}_B F = \overline{\dim}_B F = \log 2/\log 3$

$N_\delta(F) \le 2^k$ if $3^{-k} < \delta \le 3^{-k+1}$

$$\overline{\dim}_B F = \overline{\lim_{\delta \to 0}} \frac{\log N_\delta(F)}{-\log \delta} \le \overline{\lim_{k \to \infty}} \frac{\log 2^k}{\log 3^{k-1}} = \frac{\log 2}{\log 3} \qquad (2.19)$$

Also $\underline{\dim}_B F \ge \log 2/\log 3$

Thus, at least for the Cantor set, $\dim_H F = \dim_B F$, as it is demonstrated in Figure 2.6. In addition to these explanations, Hausdorff dimension and box-counting dimension have their own properties and they are comparable in Table 2.1. below.

Table 2.1. Comparison of Hausdorff and Box-Counting Dimension Properties

"~ "means $\overline{\dim}_B$ is finitely stable but $\underline{\dim}_B$ is not.

Properties	Hausdorff Dimension	Box-Counting Dimension
monotonicity	X	X
countable stability	X	
stability	X	~
geometric invariance	X	
Lipschitz invariance	X	X
countable sets	X	
open sets	X	
smooth manifolds	X	X
complexity	X	
practicability		X

2.4. Self-Similarity

An object can be said to be self-similar if it looks approximately the same on any scale. A self-similar object is precisely or nearly similar to a part of itself. In a way, a curve can be expressed to be self-similar if, every piece belonging to the curve, there is more and more much smaller piece that is similar to the whole curve. For instance, a side of the Koch snowflake is self-similar; it can be divided into two halves, each of which is similar to the whole, "(Hata 1985)".

Many objects in the real world are self similar, such as coastlines. They are statistically self-similar, because each part of them exhibits the same statistical properties at many scales. Self-similarity is a typical property of fractals, as it is mentioned in introduction part. In a different field of science, for example, for the design of computer networks, it also has significant results, because typical network traffic should have the self-similarity property .

2.5. Brownian Motion Self-Affinity

A fractal could be described as self-affine, if the scaling is done by different amounts in the x and y directions. By way of rescaling window, as it is seen in Figure 2.7. the self-affinity could be exihibited, "(Marques 1999)".

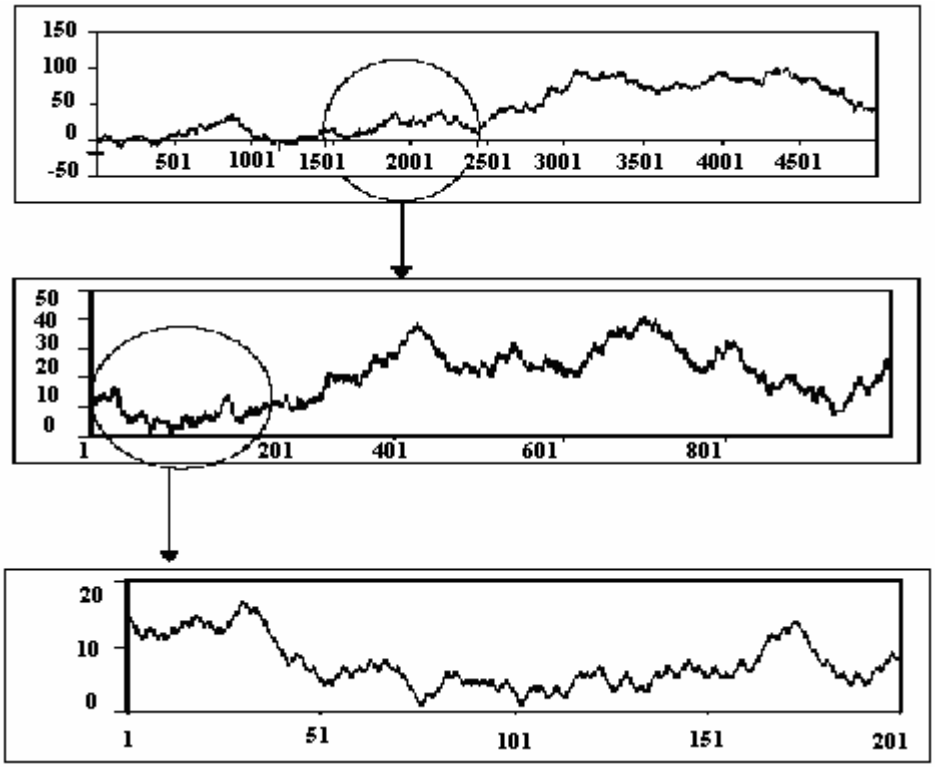

Figure 2.7. The Rescaling Window of a Measurement

Natural fractals can possess dissimilar scaling behaviours in different directions and therefore different local fractal dimensions may be required to characterize their complexity. These are multi fractals and possessing self-affinity. A particular case of self-affinity is the self-similarity, which implies isotropic transformation. For the time series, self-affine signals have to scale time and amplitude differently in order to retain its self-similar properties. The property self-affinity can be defined as wildness.

Theorem

Self-similarity is valid for all fractals nevertheless self-affinity comprise multi-fractals .

2.5.1. The Fractional Brownian Motion (fBM)

The fractional Brownian motion was introduced by Mandelbrot and van Ness (1968), who already mentioned the phenomena in hydrology or fluctuations in solids as processes to be estimated by the fBm, "(Dieker 2004)". In fact, the essential thinks were the experimental results of Hurst for improving the fBm as an interpretation for this phenomena and his finding is essential for a lot of natural time-series and this given relation was legitimate :

$(R/S) \propto \Delta t^{-H}$

where R is the maximum range (= max - min) of the summed differences of the time series and *S* the standard deviation. H is referred to as the Hurst parameter or the parameter of self-similarity, "(Hutchinson 1981)". Mandelbrot and van Ness (1968) defined the fractional Brownian motion as follows:

$$B(t,\omega) - B(t_0,\omega) = \frac{1}{\Gamma(H+1/2)} \left\langle \int_{-\infty}^{0} [\ (t-s)^{H-1/2} - (-s)^{H-1/2}\ ]\, dB(s,\omega) + \int_{0}^{1} (t-s)^{H-1/2}\, dB(s,\omega) \right\rangle$$

where $\Gamma(x)$ is the gamma function and $B_H(0,\omega)$ b_0. Mostly this initial condition is 0, "(Scheffer and Filho 2001)".

2.5.2. An Essential Codimension, Hurst (Hölder) Exponent

As it is mentioned above, H is a codimension or Hölder (Hurst) exponent, discovered by the mathematician, H.E. Hurst, is now could be expressed as the "roughness exponent" by metallurgists. H.E. Hurst is a hydrologist, worked on a project, concerning the Nile river in the 1960s. His comparing method of the inflow and outflow of the Nile over many years was the most suitable statistical model of classifying series of data in connection with correlations between past and future events

and including different time scales. Re-scaled range analysis is the skeleton of its statistical measurement, which shows the degree of non-randomness intrinsic in a system. Two situations can be observed according to changing Hurst exponent values. A series of data are persistent if the Hurst exponent is calculated of value greater than 0.5 and anti-persistent under the condition, the Hurst exponent is less than 0.5. The fractal dimension, namely the Hausdorff dimension D, of a system with Hurst exponent H, can be calculated through this simplest equation;

$$D = 2\text{-}H \tag{2.20}$$

2.5.3. Combination of Fractional Brownian Motion and Hurst Exponent

In order to retain the self-similar properties of the Brownian motion trace the axes need to be scaled differently. As it is recognized from the Figure 2.8. below the time coordinate and the spatial coordinate were scaled in different manners. The first one was scaled up four times as long as the other one was scaled only by a factor two.

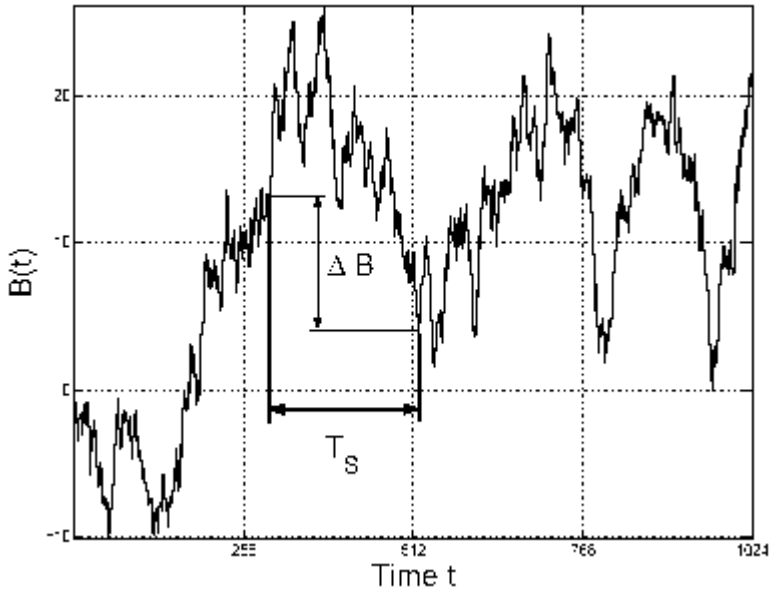

Figure 2.8. The Scaling Relationship

By sliding a window of length T_S over the trace the mean absolute separation in B(t) may be calculated by averaging the absolute difference, ΔB, for each slide step. The scaling relationship between the mean absolute separation along the fBm trace and the time of the separation is expressed as

$$\left| \overline{\Delta B_H} \right| \propto T_S^H \tag{2.21}$$

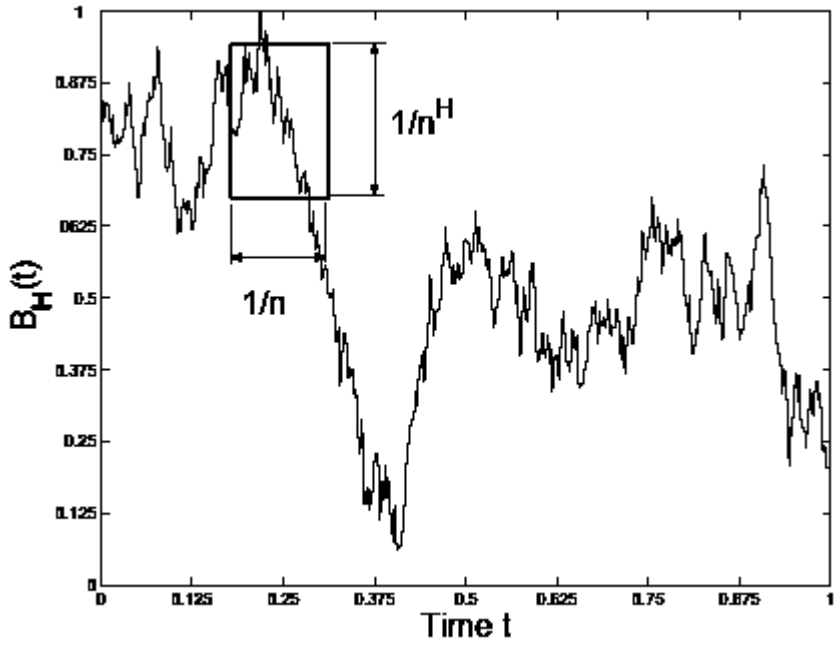

Figure 2.9. Scaling t by a Factor 1/n.

It demands a scaling of $B_H(t)$ by a factor $1/n^H$. In other words, this scaling property, concerning the relationship between fractional Brownian motion and the Hurst exponent in order to spend a zooming facility by mean of self affinity, it is clear in Figure 2.9, "(Hasfjord 2004)".

So that estimating the box counting dimension of a Brownian motion trace, the trace needs to be covered with boxes. On the other hand, due to the self- affine nature of the trace, the trajectory would not be self-affine and the height and base of the boxes needs to be scaled differently.

2.6. Multi-Fractals

This section provides a general introduction to multifractality. Chaotic, turbulent-like systems that belonging in different physical systems, have a chance to be explained through multifractal property. Multifractality is usually presented as intensive, scalar variables of nicely specified physical definition and chaotic structure. Generally, multifractality is proved by its statistical characteristic and it is demonstrated as a multiscaling, power-law behaviour. As mentioned earlier in the part of "self-affinity", natural fractals can possess dissimilar scaling behaviours in different directions and therefore different local fractal dimensions may be required to characterize their complexity.

CHAPTER 3

EXAMINATION OF TIME SERIES VIA FRACTAL GEOMETRY

Simple deterministic non-linear systems can lead to complex behaviour, which is statistically indistinguishable from that produced by a completely random process. One obvious outcome of this is that it may be possible to depict clearly complex signals using simple non-linear models. This gives the chance to develop a variety of novel techniques for the manipulation of such chaotic time series. In some situations, fractal geometry calculations are able to attain highly good performance.

Customarily, the darkness of the science "uncertainty" has been modelled using probabilistic methods, it means that it was done by combining both random variables and processes in the same model. On the other hand in this thesis the concept of the fractal geometry, especially fractal dimension calculation to measure the complexity of ECG time series of observed data, obtained from various sensors, is used.

3.1. A View to Non-linear Time Series in the Field of Fractals

Mathematicians, scientists and engineers realized that uncertainty could also be produced in certain proper conditions by purely deterministic mechanisms. This phenomenon was revealed to be known as "chaos" and is primarily due to the capacity of many nonlinear dynamical systems to rapidly amplify an insignificant amount of uncertainty about the initial state of a system into an almost total lack of knowledge of its state at a later time.

3.2. Applications of Fractals and Fractal Geometry

Because of being chaotic, time series could not be modelled by common non-linear dynamics techniques. On the other hand all the areas, where these techniques are in use, are convenient to apply the fractal geometry measurements. For instances, diagnostic monitoring of engineering systems such as turbines, generators, gear-boxes. These all undergo complex deterministic vibrations and it is often important to detect as early as possible slight changes in their operating behaviour which indicate some malfunction such as a shaft, turbine blade or gear tooth beginning to crack. Similarly many biological systems exhibit highly deterministic nonlinear oscillations, e.g. the heart beat ECG, circadian rhythms, certain EEG (Electroencephalogram) signals etc.

In many different branches it is possible to meet these techniques. For example, agglomerated properties of populations can in some circumstances show strongly deterministic features. Apart from obvious applications such as forecasting the transmission and development of epidemics, there is also interest developing and validating models of ecological systems and their interaction with man.

Substantial effort can also be exhibited in applying these techniques to financial and economic data such as foreign exchange rates and stock market indices. It appears as though the behaviour of such systems has more structure than can be explained by traditional linear stochastic models.

As it is explained ebove fractals and fractal geometry have different various scientific fields to apply. In addition to these explanations some areas, in which fractals and fractal geometry used exactly, should be expressed in a detailed manner in order to demonstrate the significance of this new method, using fractals and fractal geometry.

3.2.1. Medical Applications of Fractals

As a matter of fact, medicine is direct area to use fractals and fractal geometry. Direct because, almost the nature all of the creatures seems to be fractal and therefore can be explained only through fractal geometry, where the Euclidean geometry remains inappropriate to describe them. Such as histopathology, which is concerned with the study of the morphological changes in cells and tissues during disease. These changes

take place at the microscopic or submicroscopic degree. Histopathology assists to clarify histological images to make a diagnosis and selection of treatment.

The analysis and description of such complex and not symmetrical morphologies is hard because of being qualitative and subjective. Fractal geometry can get rid of these problems by providing new approaches to objective measurement and understanding of shape complexity and it can enable to model and understand many physical and natural process that previously were considered irregular and patternless. Here in this level it is meaningful to mention about autocorrelation, because time series, which is expressed as complex, is used in this thesis and autocorrelation function was utilized in order to find the correlation dimension to analyze its complexity.

3.3. Autocorrelation

Autocorrelation function is a time dependent function, which is identical, considering its time shifted replica, for all values of t. In other words, the autocorrelation function measures the average magnitude of the correlation of two points separated in time with a lag t. This function has a maximum at t = 0 which shows clearly that a function is most similar to itself when it has not been time-shifted, "(Web_2 1993)". When there is no correlation in the time series then the expectation value of correlation function is zero.

Autocorrelation function is computed by the formula:

$$A(\tau)=\frac{\sum_{i=1}^{N-\tau}(x_i-\bar{x})(x_{i+\tau}-\bar{x})}{\sum_{i=1}^{N-\tau}(x_i-\bar{x})^2}, \qquad \bar{x}=\frac{1}{N-\tau}\sum_{i=1}^{N-\tau}x_i \tag{3.1}$$

x_i represents ith element of the series, τ is time delay (Optimal time lag) and N is equal to length of the series. τ is determined from the shape of the correlation function, as the position of its first decrease under 1/e or 1/10, "(Miksovsky and Raidl 2001)" and this value is used to find the embedded dimension in phase space, which gives the correlation dimension value.

3.3.1. Autocorrelation of Fractal Functions

This theme is almost the backbone of this thesis, because the functions related to autocorrelation are directly the main way in order to estimate the fractal dimension by means of power law relations.

As it was remarked, quantities varying with time often turn out to have fractal graphs. One way in which their fractal nature is often manifested is by a power-law behaviour of correlation between measurements seperated by time h.

A measure of the correlation between f at times seperated by h is provided by the autocorrelation function

$$\text{C(h)} = \lim_{T\to\infty} \frac{1}{2T} \int_{-T}^{T} (f(t+h)-\overline{f})(f(t)-\overline{f})dt$$

$$= \lim_{T\to\infty} \frac{1}{2T} \int_{-T}^{T} f(t+h)f(t)dt - (\overline{f})^2$$

It could be seen that C(h) is positive if $f(t+h)-\overline{f}$ and $f(t)-\overline{f}$ tend to have opposite sins. If there is no correlation, C(h)= 0.

Autocorrelations provide several methods of estimating the dimension of the graph of a function or signal f. The autocorrelation function $C(h)$ or equivalently, the mean-square change in signal in the time h over a long period could be computed, and so

$$2[C(0)-C(h)] \cong \frac{1}{2T} \int_{-T}^{T} (f(t+h)-f(t))^2 dt$$

If the power-law behaviour

$$C(0)-C(h) \cong ch^{4-2s}$$

is observed for small h, it might be expected that the box dimension of graph f to be s. In other words,

$$\dim_B graph \quad f = 2 - \lim_{h \to 0} \frac{\log(C(0) - C(h))}{2 \log h}$$

if this limit exists.

It should be known about $C(0)$-$C(h)$ for small h; typically this depends on the behaviour of its transform $S(\omega)$ when ω is large. The situation of greatest interest is when the power spectrum obeys a power law $S(\omega) \sim c / \omega^{\alpha}$ for large ω, in which case

$$C(0) - C(h) \sim b h^{\alpha - 1}$$

for small h, for some constant b.

Comparing these equations

$$C(0) - C(h) \cong c h^{4-2s} \qquad \text{and} \qquad C(0) - C(h) \sim b h^{\alpha - 1} \quad ;$$

suggests that graph f has box dimension s where 4-2s = α-1, or $s = \frac{1}{2}(5-\alpha)$. Thus it is reasonable to expect a signal with a $1/\omega^{\alpha}$ power spectrum to have a graph of dimension $\frac{1}{2}(5-\alpha)$, "(Falconer 1990)".

3.4. The Purpose of Existence of Fractional Dimensions

Fractal analysis is a proper way to apply to a variety of research fields to characterize highly irregular and nonstationary data. Showing a time series fractal properties, its self-similarity can be described by the fractal dimension value D. For the fractal dimension estimation usually a complex rectification procedure is demanded.

3.5. Fractal Analysis of Time Series

In this thesis also the correlation method was used to find the fractal dimension. Actually it seems something different from examined two fractal dimension calculation methods, whereas the main idea is almost the same. Other fractal dimension calculation methods, exactly the box-counting method and roughly the Hausdorff method are also examined. In the lightening of these examinations it is clear that fractal analysis can bring a new insight to other signal processing methods, concerning reliable system characterization under changing external conditions.

3.5.1. Correlation Method

Gaussian probability density functions give the facility to describe the investigated time series as stochastic processes by means of consequential time-series analysis methods. Moreover, through calculating the power spectral density functions by the commonly used FFT algorithm, it could be supposed that the time series is stationary. These assumptions are quite restrictive and they are rarely met in real life. Fractal analysis methods do not make such assumptions and in addition to do this, they can supply different kinds of solutions to the emerging difficulties. Here the major steps of the analysis are outlined. It can be approximated by the correlation function that we have already encountered. Instead of analyzing what happens when we shrink covering sets, this function measures the distance between each pair of points in a space and then counts all the pairs which fall within a specified radius. (See Figure 3.1.) When we expand the radius to include all the points of interest, we have a good idea about the structure of the space.

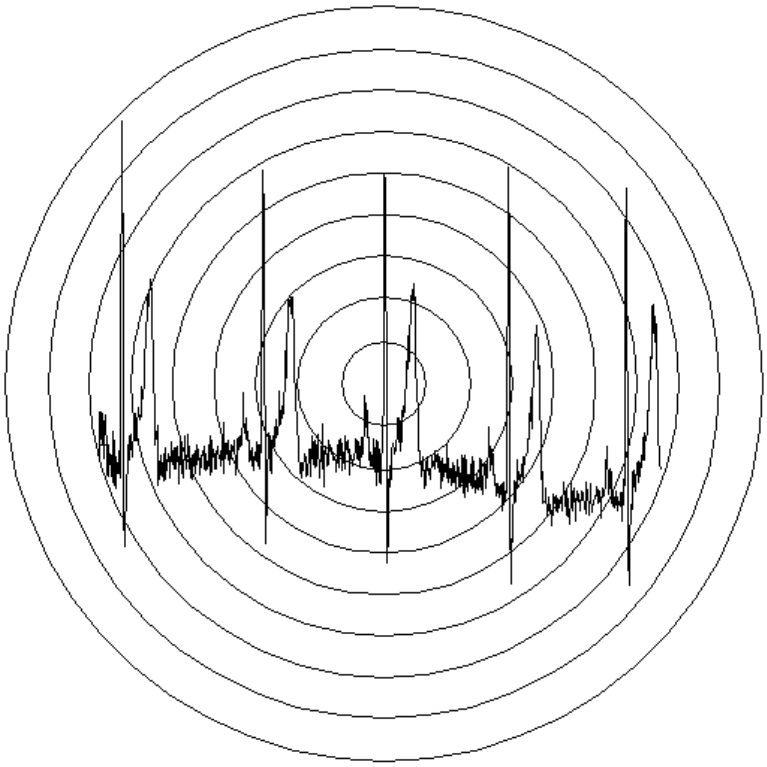

Figure 3.1. Correlation Dimension Designation

Obtaining of correlation dimension is applying the same idea as the Hausdorff dimension. But there is an exception due to using circles instead of squares. Let R be the radius of the circle and let N(R) be the number of pixels that were occupied within the radius of the circle. The correlation dimension is then defined by: $\mathbf{N(R) \sim R^C}$ where C is the correlation dimension. Taking the logarithm of both sides will give an equation that matches the form of the equation for a line: **logN = C logR** so that with several different size of circles and plotting logN versus logR the slope of the line will express the correlation dimension, "(Ringler and Roth 2002)".

3.5.2. Hausdorff Method

To determine the Hausdorff dimension of a space, we must then determine whether this measurement diverges to infinity as we shrink d, that is, as we make our collection of covering sets smaller and smaller. It happens that there is a unique value for s where this value will not diverge, and that determines the Hausdorff dimension.

$$\dim_H F = \inf\{s: H^S(F) = 0\} = \sup\{s: H^S(F) = \infty\}$$

$$H^S(F) = \left\{ \begin{array}{ll} \infty \ , \ \text{if} & s < \dim_H F \\ \\ 0 \ , \ \text{if} & s > \dim_H F \end{array} \right\} \text{ Think of s as a variable between } 0 \leq s \leq n .$$

(See Figure 2.5. in Chapter 2)

Obviously, but unfortunately, direct calculation of the Hausdorff dimension is often intractable. There is no formula, Hausdorff measure of a set can be considered as a measure that covers this set using balls of different diameter. This the similar idea to that of the box-counting dimension, however in the case of the Hausdorff measure the balls covering the set vary in diameter.

Hausdorff dimension has the advantage of being defined for any set, and is mathematically convenient, as it is based on measures, which are relatively easy to manipulate. A major disadvantage is that in many cases it is hard to calculate or to estimate by computational methods. Therefore in this thesis, the Hausdorff dimension was calculated using the formula D_H = 2- H, including the Hurst exponent H, through the package software "Fractan" (From Institute of Mathematical Problems of Biology RAS).

3.5.3. Box-Counting Method

Fractal dimensions are important quantities in characterizing the geometric structure of strange sets. In particular, they provide measures of the arbitrarily fine scale structure of invariant sets generated by chaotic processes. From a practical point of view, they also provide an estimate of the minimum number of degrees of freedom needed to describe the dynamical evolution of these chaotic systems. One of the simplest and most intuitive definitions of the fractal dimension of a strange set is the box-counting dimension D_B .

Given a fractal set in a d-dimensional Euclidean space, D_B gives the scaling between the number of d-dimensional ε boxes needed to cover the set completely, and the boxes' size ε, "(So et al. 1999)".

$$D_B = \lim_{\in \to 0} \frac{\ln(N(\varepsilon))}{\ln(1/\varepsilon)} \tag{3.2}$$

Direct application of these geometric definitions to chaotic dynamical systems is difficult, since as ε decreases it becomes impossible to determine all the ε boxes visited by a given trajectory from a finite amount of data. This problem is especially severe for the box-counting dimension, because it can depend heavily on regions infrequently visited by a typical trajectory.

3.6. Box-counting Dimension Calculation

A time series is plotted through a small code in matlab, using the data of observed specimen. This signal is recorded according to a sampling interval, concerning the starting and ending times in seconds until reaching at the proper sample size. This method could be applied to various kind of signals. For instance an ECG signal in Figure 3.2. was held to demonstrate the usage of box-counting method in order to estimate the dimension of the signal. In Figure 3.2., x-axis shows the sampling time in seconds and the y-axis shows the unit in milivolts.

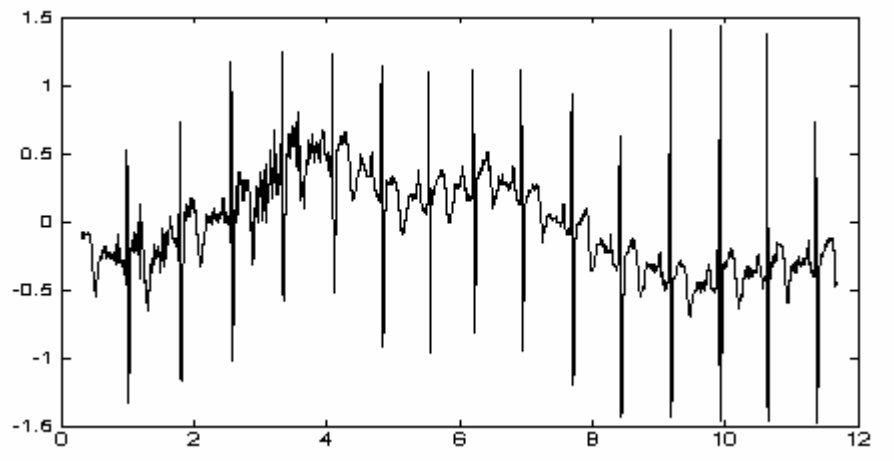

Figure 3.2. An ECG Time Series

For this ECG time series

- sampling interval is 1/180 second
- starting time is taken to be 0.31 seconds
- ending time is taken to be 11.6822... seconds
- units for this time series are in millivolts
- sample size is 2048

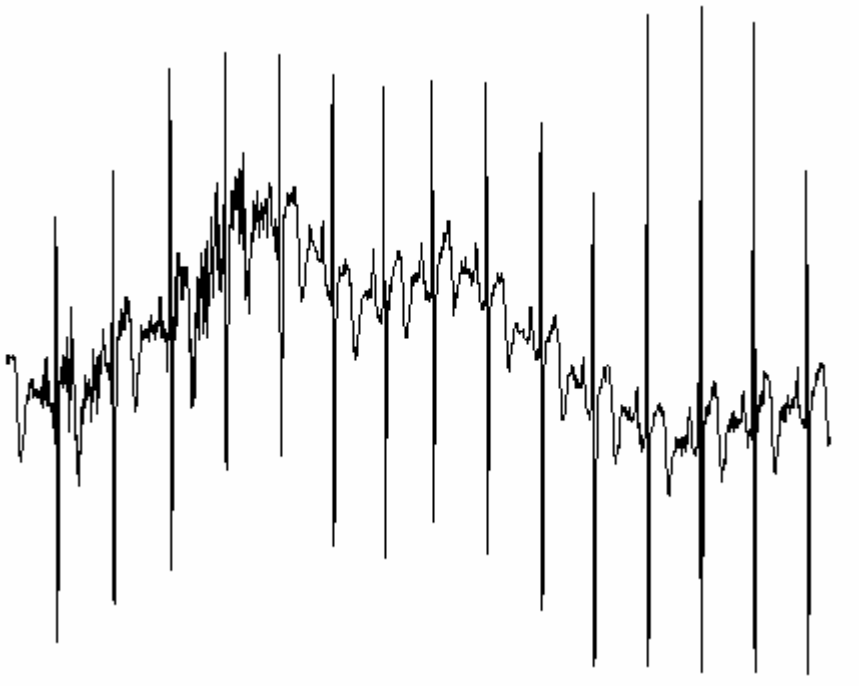

Figure 3.3. ECG Signal in bmp Form

Recorded ECG signal was converted into the “bmp” form, as it is seen in Figure 3.3., in order to use fractal dimension calculator. [From Bar-IIan University] This fractal dimension calculator uses box-counting method, as it is given in the definition, the signal was covered with boxes of the same size.

During this stage, it is very significant to care about how to make the covering, because the whole signal should be covered without any dislocation. If there exist some occupying failures for the signal, the calculated box-counting dimension loses indirectly its accuracy. In other words, being less or more boxed of the signal, change the value of the dimension, because number of boxes affects clearly the estimation of dimension, it can be seen from the box-counting dimension formula in a direct manner. On the other hand there are some confusions, thinking about the efficiency of the boxcovering. Also the cover-style can play a role in changing of the value of dimension. It means that different boxing types create different box numbers. This change results from the lacunas, occuring in the boxes. Counting the boxes without caring about the emptiness in them is the same approach as counting money without caring about the value of banknotes and this reason points at also mis-computation of the box-counting dimension.

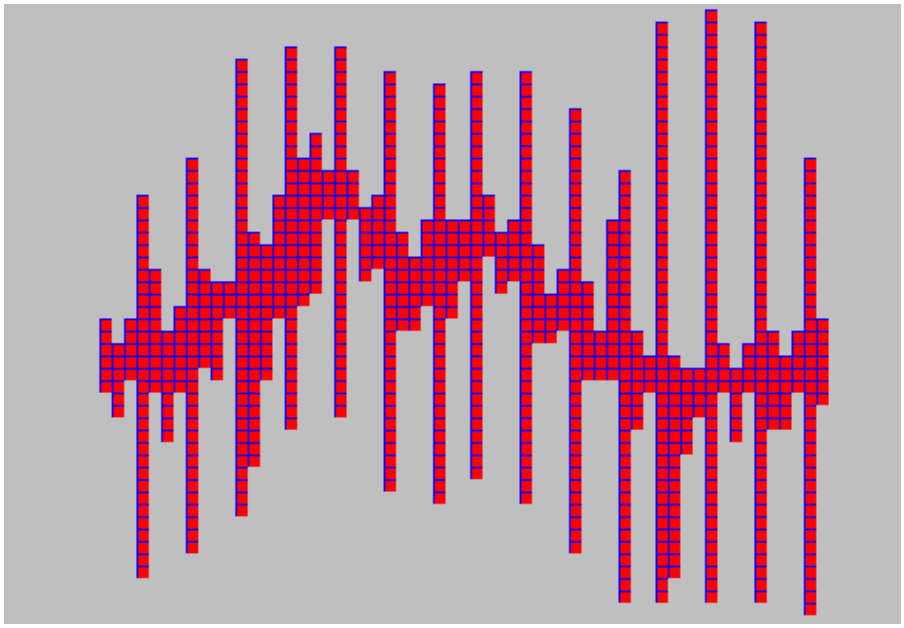

Figure 3.4. After Covering ECG Time Series With Boxes

This example gave a covering as it is seen in Figure 3.4. At this measurement 865 boxes size of 7 were obtained. In order to make accurate measurement, different box sizes were used. According to changing box sizes various number of boxes were calculated and it was demonstrated in Table 3.1.

Table 3.1. Box Sizes and Counted Boxes

Box-size	**1**	**2**	**4**	**6**	**7**	**8**	**25**	**59**	**60**	**86**	**127**
Box #	**10627**	**4294**	**1771**	**1065**	**868**	**772**	**173**	**42**	**39**	**22**	**11**

These data given above in the table were used to be able to plot a regression line. Taking the general fractal dimension formula, the logarithmic N(E) values and the logarithmic E values have a linear relationship, if we consider these values in a coordinate system. The formula of fractal dimension D_B is below;

$$D_B = \frac{\log N(E)}{\log E} \tag{3.3}$$

The linear relationship takes place in the coordinate system, showing the logarithmic N(E) values on the y-axis and the logaritmic E values on the x-axis. (Plotted regression line can be seen in Figure 3.5.). The regression line results from this linear relationship, in other words if there is a linear relationship, there is also the facility to find the optimal box number to calculate the box-counting dimension.

In this step, data coming from the package program, including box sizes and box numbers, were used in order to calculate the box-counting dimension. This program provides data in different box-sizes and box-numbers. These data were composed with a well-known method, named “Simple Linear Regression” especially “Least Square Method”, which is an useful and popular technique in the field of statistics, to find the box-counting dimension via the slope of the regression line.

3.6.1. Determination of Regression Equation

A proper way to express the relationship between two group of variables is, building a line, including all data.
Its primitive mathematical formula is;

$$y = a + bx \tag{3.4}$$

On the other hand statistics has developed this formula and defined in a different form. In order to obtain the predicted regression line equation, firstly the error term of the model should be examined and it was given in the formula below.

$$e = y - \beta_0 - \beta_1 x \tag{3.5}$$

For all observations, square of this term could be defined so

$$\sum_{i=1}^{n} e_i^2 = \sum_{i=1}^{n} (y_i - \beta_0 - \beta_1 x_i)^2 \tag{3.6}$$

For the least square method, b_0 and b_1 are the predicted values of β_0 and β_1, which give the smallest value to the result of the equation above. If this equaton will be derivatized according to β_0 and β_1, and then calculated, concerning it will be equal to zero, the predicted value of β_1 will be equal to b_1, which can be expressed as,

$$b_1 = \frac{\sum xy - \frac{(\sum x)(\sum y)}{n}}{\sum x^2 - \frac{(\sum x)^2}{n}} \tag{3.7}$$

and the predicted value of β_0 will be b_0, which is equal to this formula.

$$b_0 = \bar{y} - b_1 \bar{x} \tag{3.8}$$

The equation of the regression line, that is the best fit to data, could be described as,

$$\hat{y} = b_0 - b_1 x \tag{3.9}$$

where $\hat{y}$ is the predicted value of y, "(İkiz et al. 2000)".

Estimation of regression equation requires some simple calculations, for instance, $\sum xy$, $\sum x$, $\sum y$, $\sum x^2$, $(\sum x)^2$, $\bar{x}$, $\bar{y}$ should be done necessarily to construct the equation, through finding b_0 and b_1 values. (These calculations were made through excel program) As another step, plotting the regression line is the quality of being absolutely essentialnes, because of demostrating, how to fit the choosen points in pairing of box-size and box-number to the regression line. On the other hand the box-counting dimension could be found without plotting the regression line. This reasoning results from the simple box-counting dimension equation, according to the fact that the expected value of the equation exhibits the idea, which is that the slope of the regression line could give the box-counting dimension. In the lightening of this expression, the box-counting dimension value can be obviously seen from the regression equation, because it is a linear equation and the value of b_1 gives the slope of the regression line, exactly being equal to the value of box-counting dimension. It can be seen also from the mathematical form of fractal dimension formula.

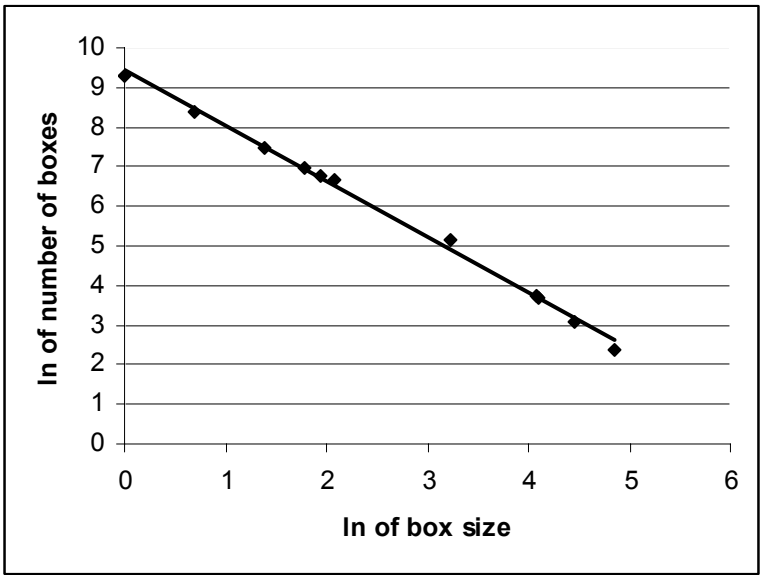

Figure 3.5. The Regression Line Plot

In order to be able to use the package program, the signal should be converted into bmp form, because this program permits to process signals only in this form. It does not allow any colored format except from the black-white. By way of this program the signal was covered with boxes. Box sizes were randomly selected and box numbers were automatically computed. Tables were organized, including defined box sizes and box numbers, belonging them to simplify seeing data together. Unfortunatelly these measurement results could not be used concerning the box-counting dimension formula, because logarithmic values should be calculated, in order to obtain accurate box-counting dimension value.

3.7. Demonstration of Accuracy of Fractal Dimension Methods

Actually, the main idea of this thesis is showing the situation of ECG time series in different states with a numerical value by way of three kinds of fractal dimension method for an easy comparison. On the other hand it is the fact that there is the need of proving the accuracy of these methods. Therefore a sinusoidal wave was examined using correlation, Hausdorff and box-counting dimensions, in the lightening of the knowledge that this sinusoidal wave should have the value of nearly one as dimension, because of having low degree of roughness. (The sinusoidal wave is seen in Figure 3.6.)

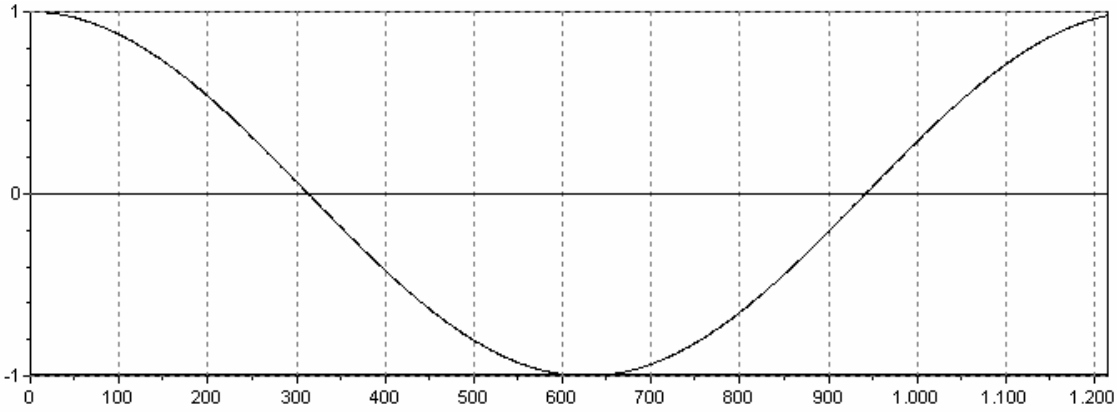

Figure 3.6. Sinusoidal Wave (Sample size: 1215)

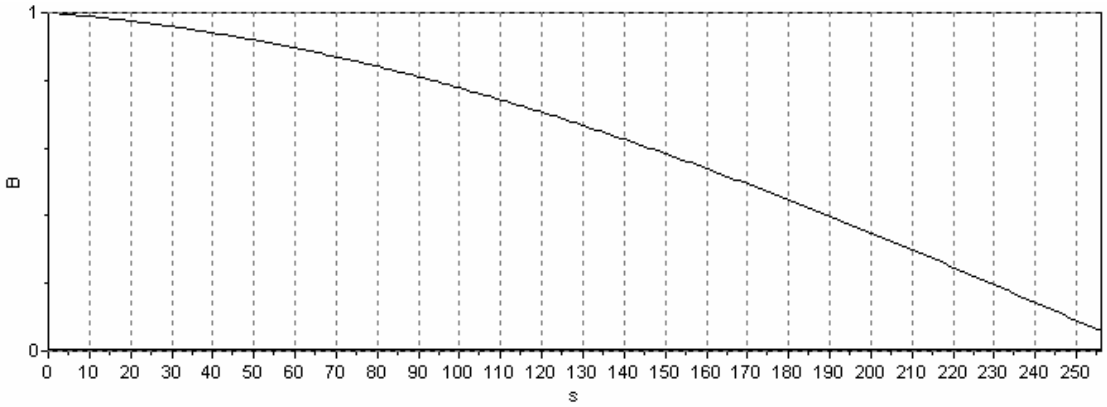

Figure 3.7. The Autocorrelation Function Graph of Sinusoidal Wave

The autocorrelation function graph of sinusoidal wave was plotted as it is seen from the Figure 3.7. and the optimal time lag has the value of 256. This optimal time lag is the key of finding the embedded dimension in the phase space and also proportionally to find the correlation dimension.

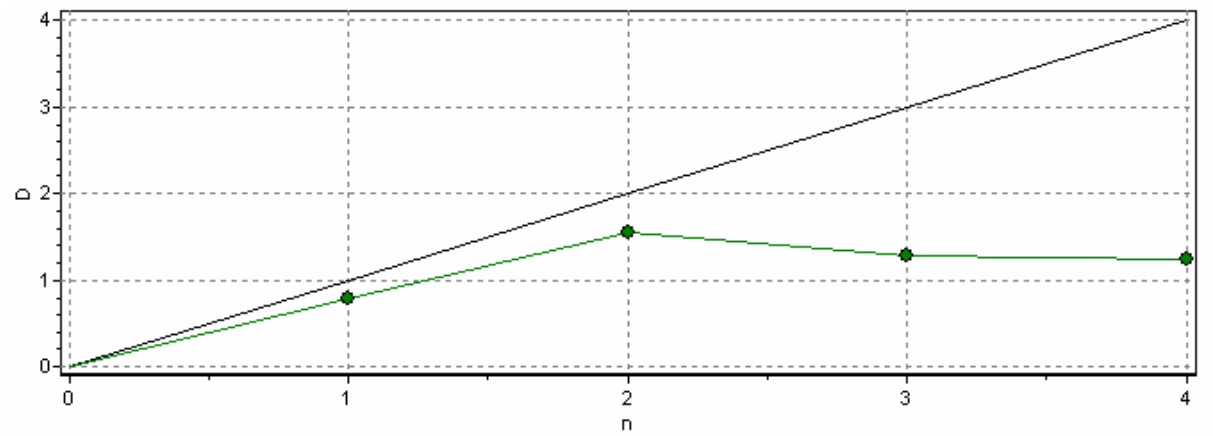

Figure 3.8. The Correlation Dimension Graph of Sinusoidal Wave

In Figure 3.8. D represents the correlation dimension and n represents the embedded dimension. Correlation dimension value is 1,551 and embedded dimension value is 2. The correlation dimension value could be seen, where the embedded dimension value makes the maximum on the y axis.

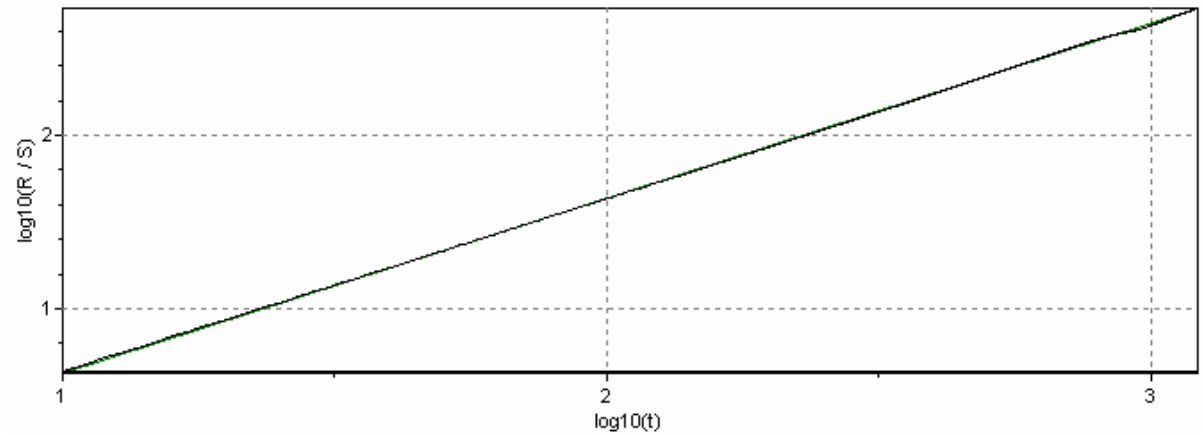

Figure 3.9. The Hurst Exponent and the Hausdorff Dimension Graph of Sinusoidal Wave

Figure 3.9. shows the Hurst exponent value, it is calculated from the slope of the line and its value is 1,0122. Hausdorff dimension value could be found using the equation “D = 2- H” and it is equal to 0,9878.

Table 3.2. Calculated Box Sizes and Box Numbers of Sinusoidal Wave

Box size	1	8	14	24	42	61	86	104	130	163	198	256
Box number	1143	185	100	62	36	24	17	12	11	10	5	4

Logarithmic values of box sizes and box numbers, as it is seen in Table 3.2., were utilized to compute the regression equation.

Regression Equation

y = 7,2358-1,0092x

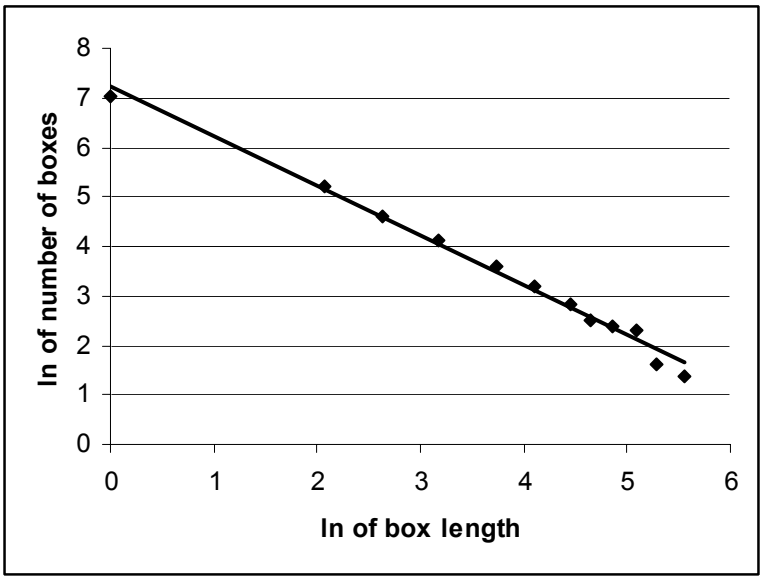

Figure 3.10. The Regression Line Graph of Sinusoidal Wave

Logarithmic values of box sizes were demonstrated on the x-axis and logarithmical box numbers on the y-axis in Figure 3.10. The slope of this regression line gives the box-counting dimension, it could be recognized also from its own formula and it is equal to 1,0092.

According to these results, two techniques indicate high degree of accuracy apart from correlation dimension, because the value of sinusoidal wave dimension should be

nearly one, concerning that the line has the Euclidean dimension value of one. Hausdorff and box-counting dimension methods gave almost accurate values, where the correlation dimension value is quite high.

In this chapter, some of the dimension calculation techniques for the detection of fractals from experimental time series have been introduced, unavoidably containing measurement and intrinsic noise, after giving short theoretical backgrounds for the methodologies. Although these methods will be shown to be useful in detecting hidden nonlinear structures in real world data, it should not be ruled out that no single technique is adequately powerful to inspect fractals with 100% confidence. Therefore in this thesis three different kinds of fractal dimension calculation techniques were used in order to reach at most accurate comparing facility.

CHAPTER 4

FRACTAL DIMENSION MEASUREMENTS AND APPLICATIONS

The heart can be thought as a system, although it is not a mechanical structure. It has its own dynamics, concerning the flow of the blood by way of muscle pumps. Like mechanical systems, the heart performance could be observed through signals, which is called ECG. From this point it is clear that to bring some approaches about dimension measurements of ECG signals in order to set a new criterion to estimate the performance of any system. Therefore in this chapter four states of three persons were examined, according to ECG signals.

These three persons were selected from the same age and height. They are in the range 23-25 years of age and 1.80-1.90 meter of height. Person-2 and person-3 are assistans at the university and the third person is a student. They are nonsmokers and carry on a systematic, healthy life. In addition, they have not any diagnosed disease. Three sensors were used to obtain the ECG signals, two of them were tied on the inside of the elbows and the other one on the inside of the wrist. Normal ECG measurements were made from six points and more detailed signals can be obtained. Another disadvantage is that measurements are noisy in unwanted manner.

Measurements in state-1 were made under normal conditions, exactly the persons were calm during measurements. On the other hand for state-2, persons were expected to walk in order to realize the effect of movement. The walk was getting rapider than the state-2, while making new measurements for the third state. Finally, three persons' ECG signals were extracted during running in order to set the state-4. These measurements were made for three persons for two applications. First application was made taking the circa 5 efficient second period, for aproximatelly 1000 samples of size of ECG signals and the second was made for the whole of the measured ECG signals. The size of the signals in application-2 are different from each other, they also were given above ECG signal graphs as information. Totally 24 signals were obtained and these signals were processed to compute/calculate fractal dimensions. The idea of comparing fractal dimensions is the lightening of using three different dimension

calculation methods, namely Hausdorff dimension method, Correlation dimension method, Box-counting dimension method.

4.1. Explanations of Graphs for Estimation of Correlation and Hausdorff Dimensions

As it was mentined earlier the behaviour of time series could be analyzed by means of autocorrelation. In other words, autocorrelation provides the consideration, how data points are correlated in a strong manner with a time lag. This time lag falls to 1/e, which is called the correlation time. It is expexted that the samples to be forcefully correlated each other with the time lag. 0 and 1 values are very significant, handling the autocorrelation function, for a zero lag autocorrelation equals to one, whereas it almost equals to zero at large time lags. (Autocorrelation function graphs were demonstrated in Appendix C). Correlation time plays a consequential role in the way of finding the correlation dimension and it can be thought as a bridge between correlation function and correlation dimension. Optimal time lag, obtained from autocorrelation function is also the time lag in embedding space, which is the way of finding embedded dimension and correlation dimension. From this view, correlation dimension is a measure of how correlated are the data points.

Hausdorff dimension is the second parameter in order to compare fractal dimensions. Nevertheless there are some difficulties in calculating this dimension because of lack of explicit formula. Therefore here the Hurst exponent was used to determine the Hausdorff dimension via calculation of this simple equation "$D_H = 2 - H$". Hurst exponent is the result of the Rescaled Range (R/S) statistic analysis. The R/S statistic is calculated for 10 equally spaced values of the time step t and for 50 logarithmically spaced values of the lag k. The slope of the line of best fit through these points gives the Hurst exponent value.

After short recalling these explanations, the analysis of ECG signals, belonging to person-1 for four states were examined here in order to determine the correlation dimension and the Hausdorff dimension.

4.2. Correlation Dimension, Hausdorff Dimension and Box-counting Methods Applications

In the third chapter detailed information about Hausdorff dimension, correlation dimension and box-counting dimension calculations were given. This part of this chapter deals with the applications of these techniques for the first person, concerning four states.

4.2.1. Application-1 for Correlation and Hausdorff Dimensions

4.2.1.1. Person -1 & State -1 (Normal)

- Sample size: 1038
- Sampling interval: 1/200 seconds
- Sampling duration: 5.185 seconds
- X-axis: Time in seconds
- Y-axis: Amplitude in milivolts

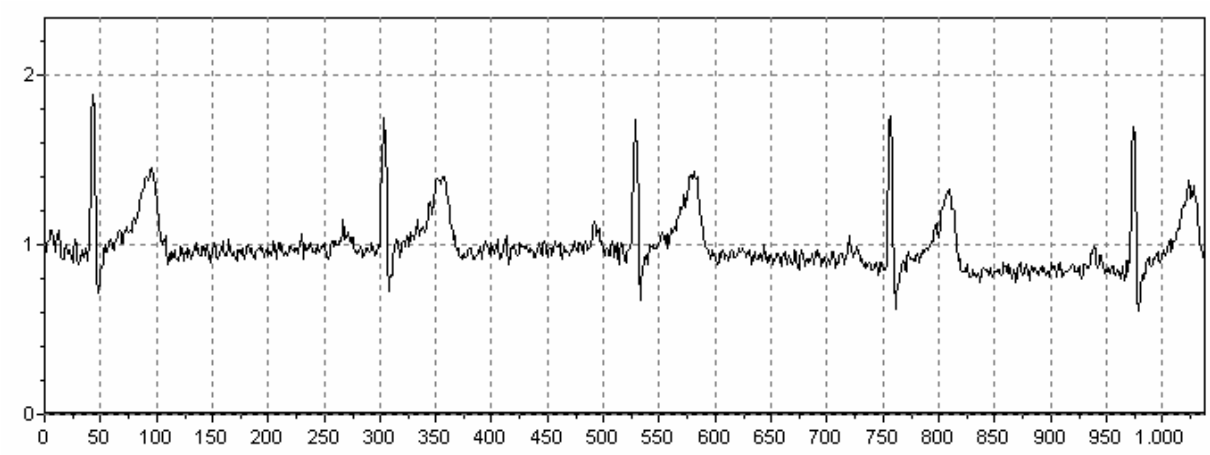

Figure 4.1. ECG Signal of Person-1 & State-1 (Application-1)

Figure 4.1. shows the ECG signal of person-1 & state-1 (Application-1). This signal seems to be deterministic as it is recognized that it repeats itself in a periodic manner. On the other hand it is the fact that the ECG signals are not completly deterministic.

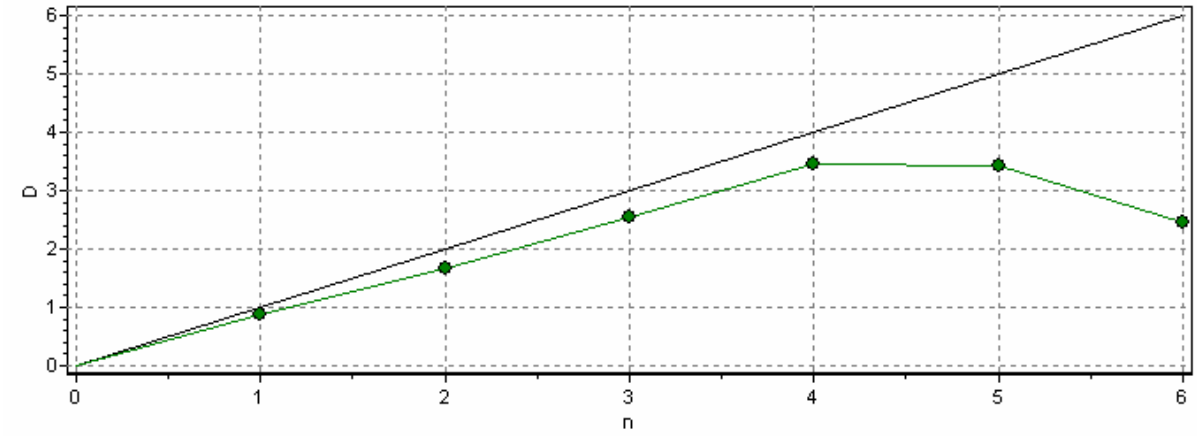

Figure 4.2. Correlation Dimension Graphic of Person-1 & State-1 (Application-1)

In Figure 4.2. D represents correlation dimension on the y-axis and n represents the embedded dimension on the x-axis. Correlation dimension value is 3.462, where the embedded dimension value is 4. Correlation dimension value is not too low, it also could be followed from autocorrelation function graphic, it rarely drops under 0 value.

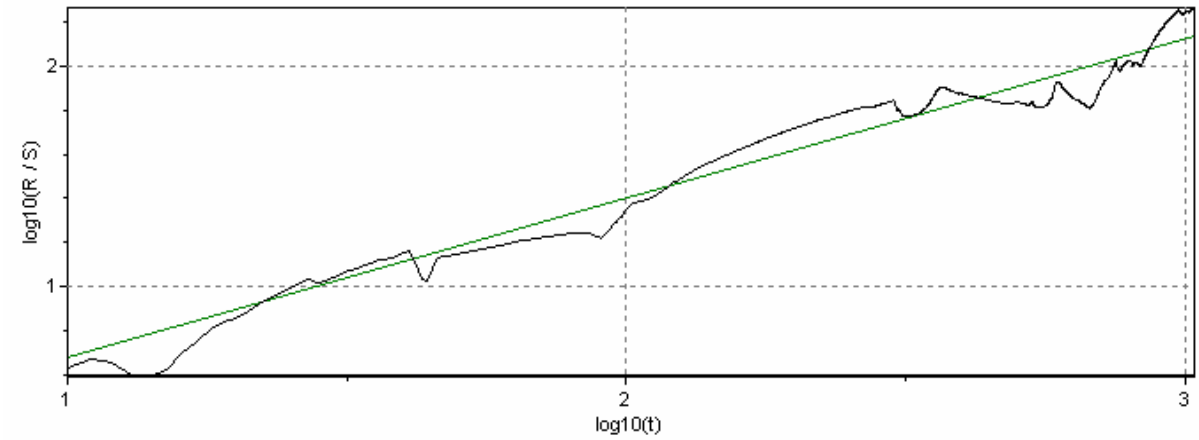

Figure 4.3. Hurst Exponent H and Hausdorff Dimension D of Person-1 & State-1 (Application-1)

Hurst exponent computation is demonstrated in Figure 4.3. and the H value is 0.7246, automatically from the equation it is easy to find the Hausdorff dimension at the value of 1.2754.

4.2.1.2. Person-1 & State -2 (Walk)

- Sample size: 1089
- Sampling interval: 1/200 seconds
- Sampling duration: 5.44 seconds
- X-axis: Time in seconds
- Y-axis: Amplitude in milivolts

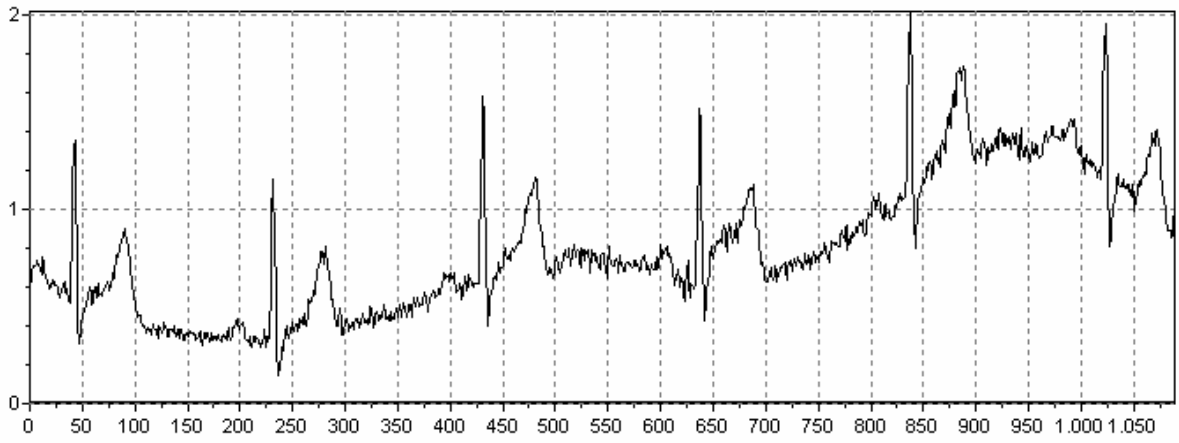

Figure 4.4. ECG Signal of Person-1 & State-2 (Application-1)

ECG Signal of Person-1 & State-2 (Application-1) in Figure 4.4. is something different as it is compared to ECG Signal of Person-1 & State-1 (Application-1). It can be realized that movements begin, concerning the undulation of the signal.

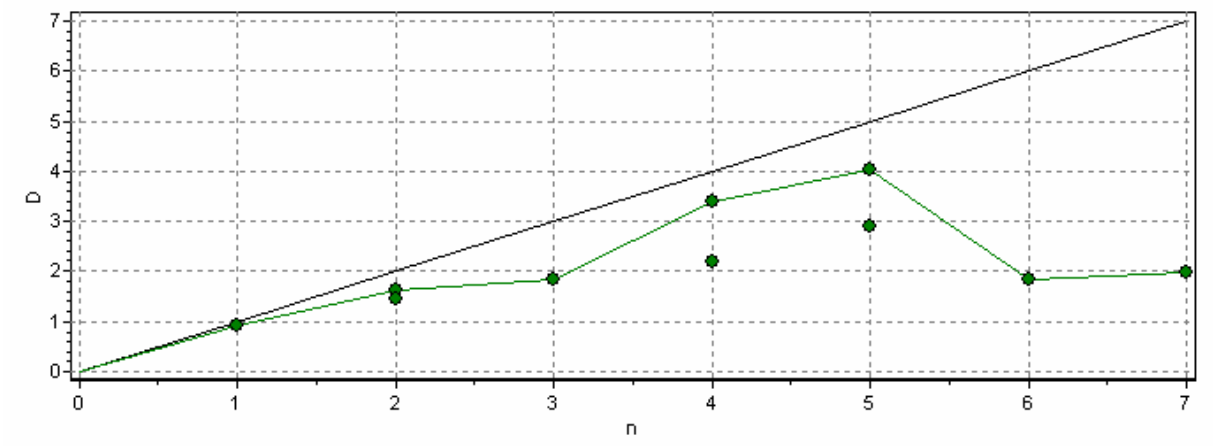

Figure 4.5. Correlation Dimension of Person-1 & State-2 (Application-1)

Correlation Dimension as D and embeded dimension as n were represented in Figure 4.5. As numerical values, correlation dimension has the value of 4.031 and embedded dimension 5. It is clear that the correlation dimension value increases in this state, the autocorrelation graphic exhibits also this increase, because the values of correlation never drop under 0.

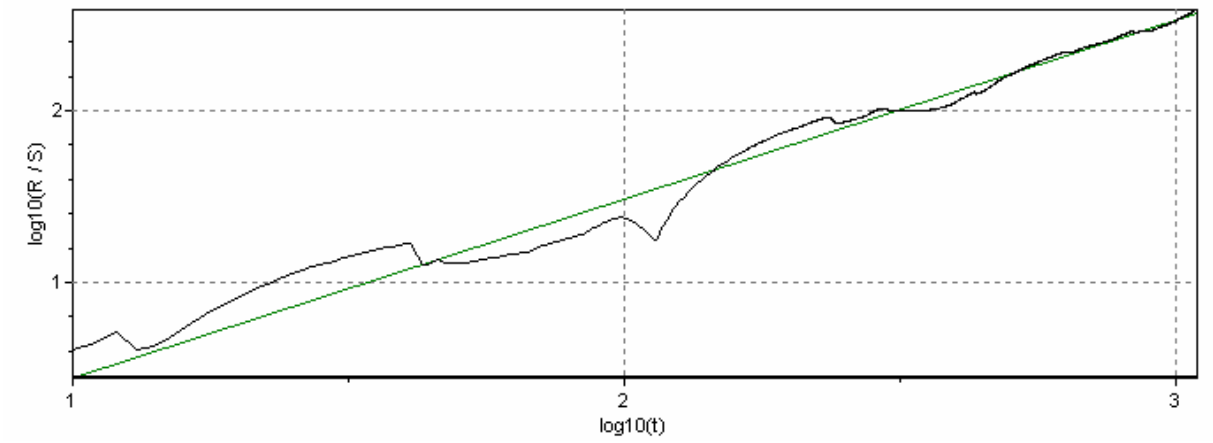

Figure 4.6. Hurst Exponent H and Hausdorff Dimension D of Person-1 & State-2 (Application-1)

The H value is 1.0482 as it was computed in Figure 4.6. and D_H is 0.9518 according to this value. Hausdorff dimension value decreases in the second state contrast to correlation dimension value.

4.2.1.3. Person-1 & State-3 (Rapid walk)

- Sample size: 1000
- Sampling interval: 1/200 seconds
- Sampling duration: 4.995 seconds
- X-axis: Time in seconds
- Y-axis: Amplitude in milivolts

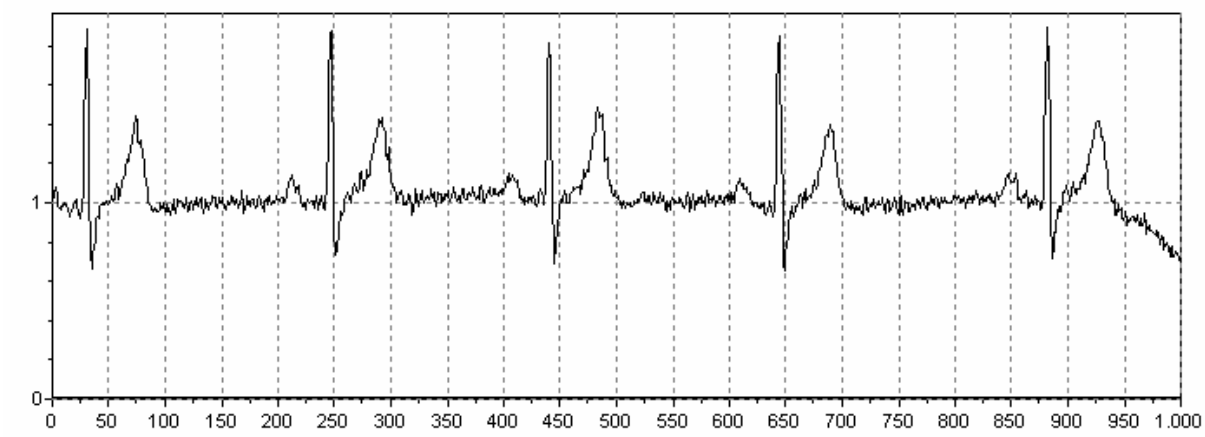

Figure 4.7. ECG Signal of Person-1 & State-3 (Application-1)

Although this ECG Signal of Person-1 in Figure 4.7. has been measured after rapid walk, it seems almost the same as the signal in state-1. It also looks periodic and normal, like in the first state. On the other hand it is obvious that the behaviour of the signal begins to change near the last samples.

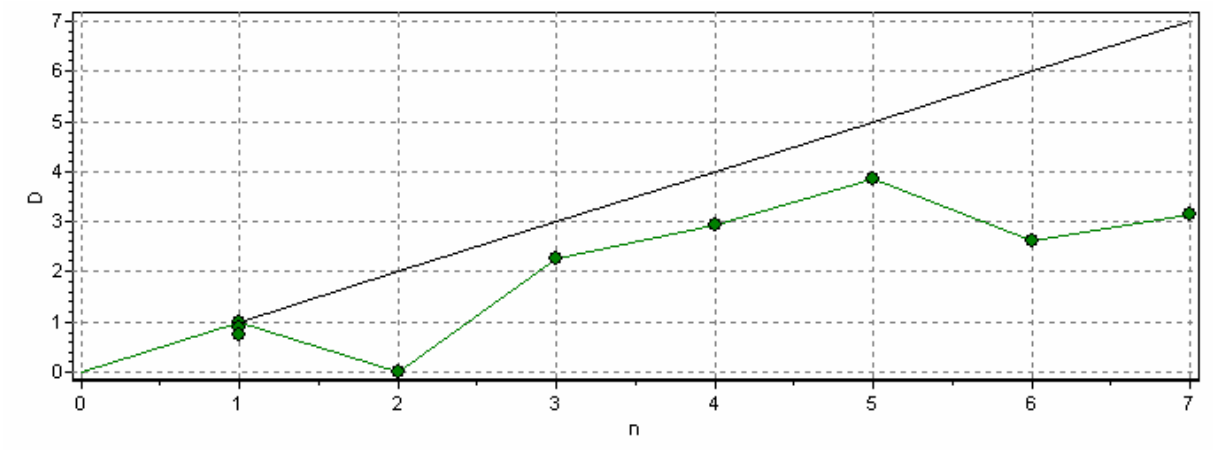

Figure 4.8. Correlation Dimension of Person-1 & State-3 (Application-1)

In Figure 4.8. D, symbolizing the correlation dimension, was measured as the value of 3.863, giving the embedded dimension n at the value of 5. Correlation dimension value is not low. Autocorrelation function graphic values drop rarely under 0.

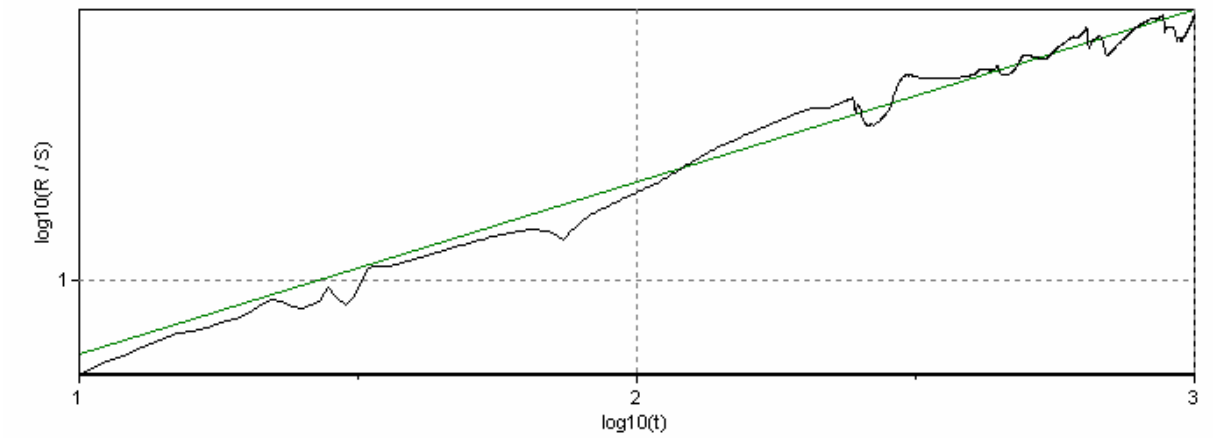

Figure 4.9. Hurst Exponent H and Hausdorff Dimension D of Person-1 & State-3 (Application-1)

According to Hurst exponent value, which was computed from Figure 4.9., Hausdorff dimension was calculated as 1.3824**,** where H was 0.6176.

4.2.1.4. Person-1 & State-4 (Run)

- Sample size: 1004
- Sampling interval: 1/200 seconds
- Sampling duration: 5.015 seconds
- X-axis: Time in seconds
- Y-axis: Amplitude in milivolts

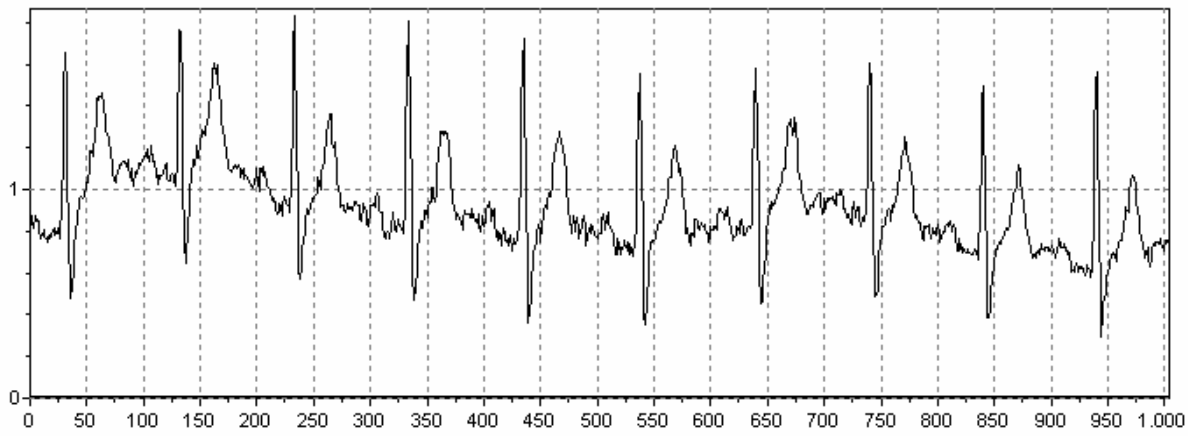

Figure 4.10. ECG Signal of Person-1 & State-4 (Application-1)

ECG Signal of Person-1 & State -4 (Application-1) in Figure 4.10. shows the period again but more frequently. In other words these perios are rather short, comparing normal state.

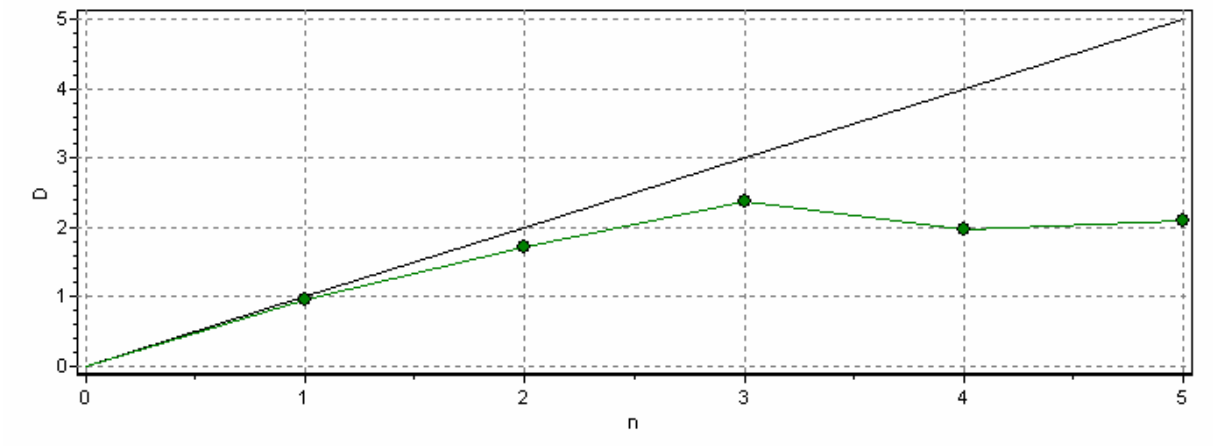

Figure 4.11. Correlation Dimension of Person -1 & State-4 (Application-1)

Correlation Dimension of Person-1 & State-4 has the value of 2.373, which is represented as D in Figure 4.11. against the embedded dimension value of 3, represented as n. Correlation dimension value decreases, concerning other three situations. Looking at the autocorrelation function graphic (See Appendix A) it can be easily realized, because the autocorrelation values have a decreasing trend.

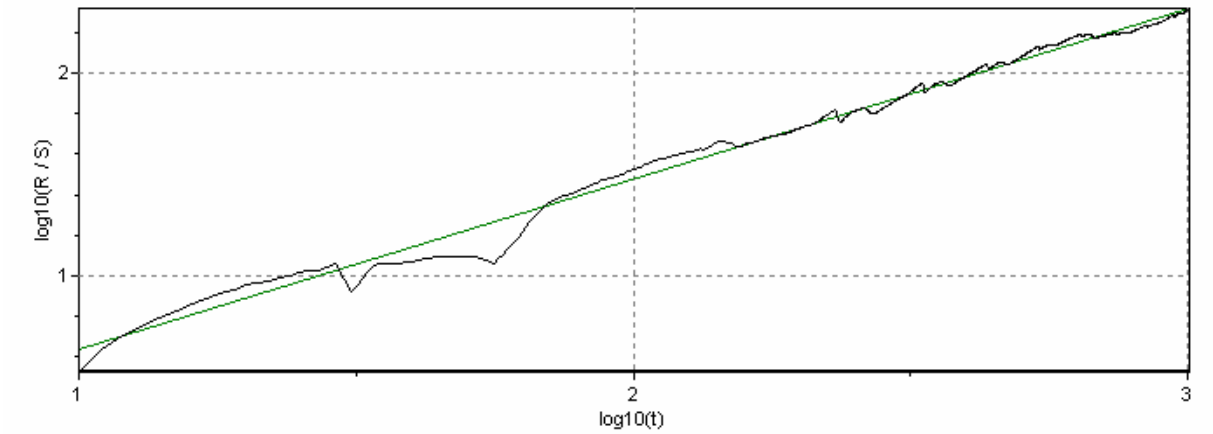

Figure 4.12. Hurst Exponent H and Hausdorff Dimension D of Person-1 & State-4 (Application-1)

As it is seen from the Figure 4.12. Hurst exponent and Hausdorff dimension values were computed. H = 0.8445, D_H = 2 – H = 1.1555. Hausdorff dimension value keeps decreasing in the fourth state like the correlation dimension value.

4.2.2. Application-1 for Box-counting Dimension

4.2.2.1. Person-1 & State-1 (Normal)

Table 4.1. Calculated Box Sizes and Box Numbers of ECG Signal of Person-1 & State-1 (Application-1)

Box size	1	7	23	52	91	120	140	167	186	205	228	251	256
Box number	7453	564	119	40	20	12	10	6	6	6	6	4	4

Regression Equation

$\hat{y} = 8{,}97 - 1{,}36x$

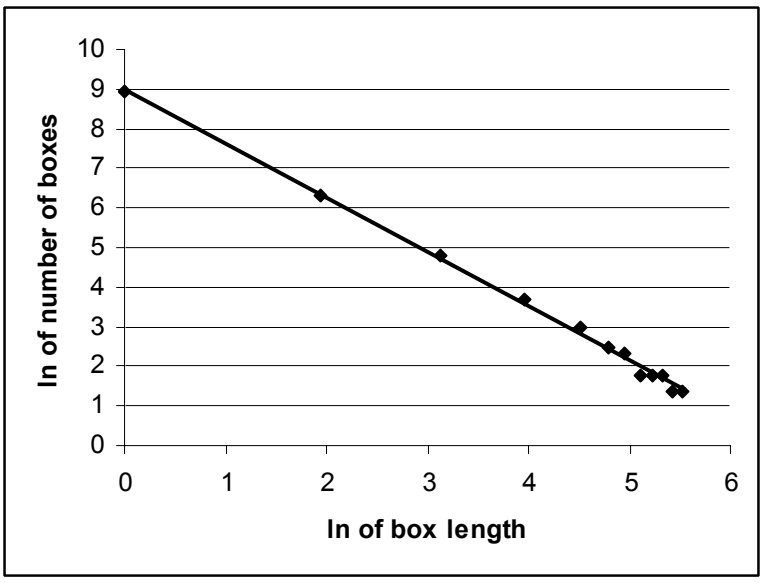

Figure 4.13. The Regression Line Graph of Person-1 & State-1 (Application-1)

4.2.2.2. Person-1 & State-2 (Walk)

Table 4.2. Calculated Box Sizes and Box Numbers of ECG Signal of Person-1 & State-2 (Application-1)

Box size	1	16	32	53	96	138	174	206	226	246	256
Box number	4817	132	56	29	12	8	6	5	5	5	5

Regression Equation

$\hat{y} = 8{,}41 + 1{,}26x$

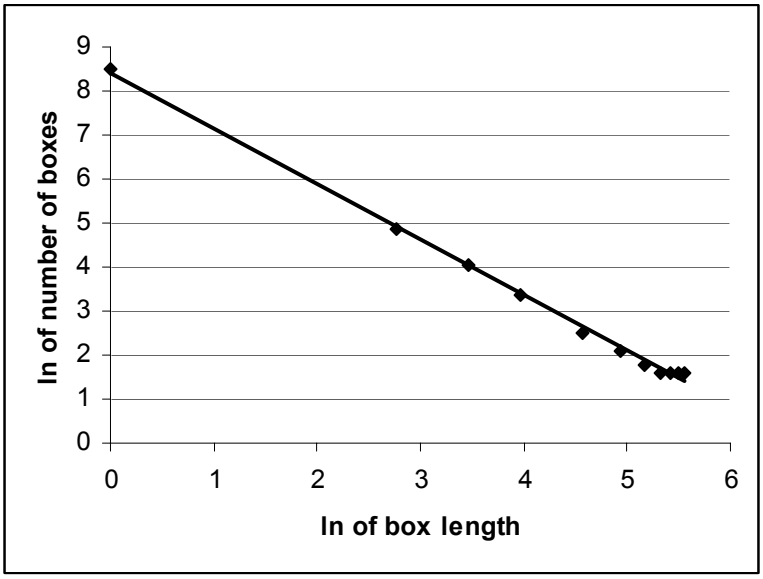

Figure 4.14. The Regression Line Graph of Person-1 & State-2 (Application-1)

4.2.2.3. Person-1 & State-3 (Rapid Walk)

Table 4.3. Calculated Box Sizes and Box Numbers of ECG Signal of Person-1 & State-3 (Application-1)

Box size	1	7	31	55	86	117	149	180	211	238	256
Box number	7016	564	81	41	27	16	9	8	6	6	6

Regression Equation

$\hat{y} = 8{,}82 - 1{,}29x$

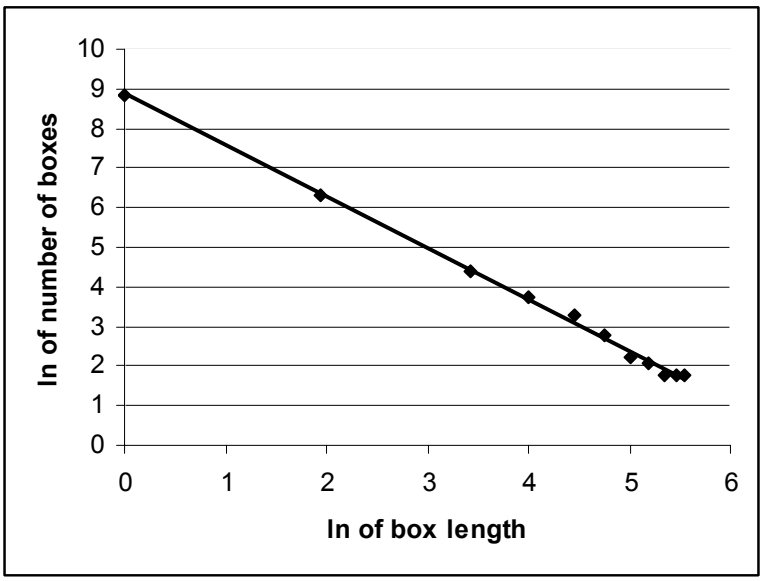

Figure 4.15. The Regression Line Graph of Person-1 & State-3 (Application-1)

4.2.2.4. Person-1 & State -4 (Run)

Table 4.4. Calculated Box Sizes and Box Numbers of ECG Signal of Person-1 & State-4 (Application-1)

Box size	1	8	16	25	36	47	74	102	135	170	207	234	251	256
Box number	7988	612	232	129	74	52	22	16	9	6	6	6	4	5

Regression Equation

$\hat{y} = 9{,}16 - 1{,}39x$

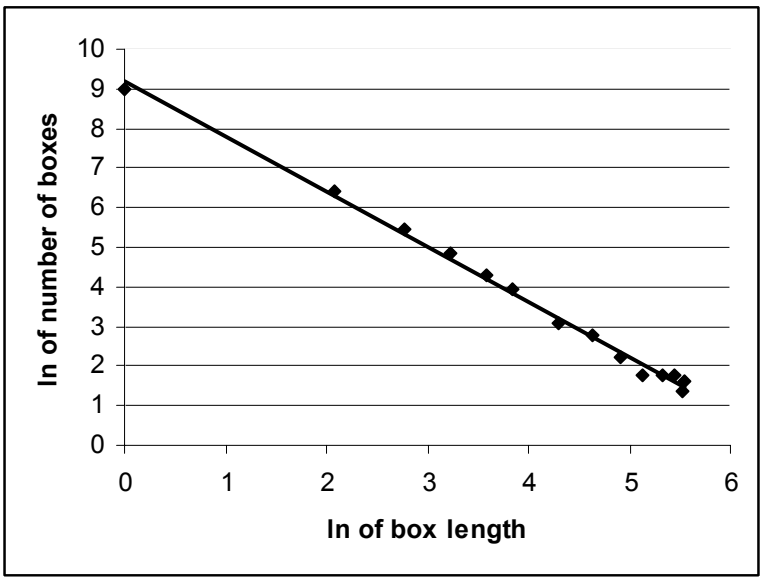

Figure 4.16. The Regression Line Graph of Person-1 & State-4 (Application-1)

4.2.3. Application-2 for Correlation and Hausdorff Dimensions

4.2.3.1. Person-1 & State-1 (Normal)

- Sample size: 11238
- Sampling interval: 1/200 seconds
- X-axis: Time in seconds
- Y-axis: Amplitude in milivolts

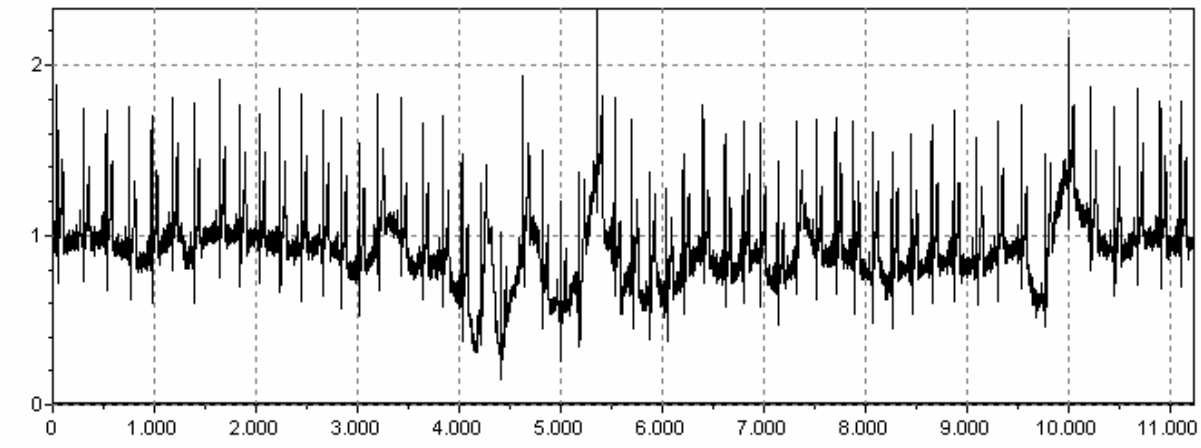

Figure 4.17. ECG Signal of Person-1 & State-1 (Application-2)

This application was made for further sample numbers and it looks more crowded than the other application measurements as seen in Figure 4.17. This is normal states signal but there are some movements during 4500-5500 sampling, resulting from persons arm actions in this period.

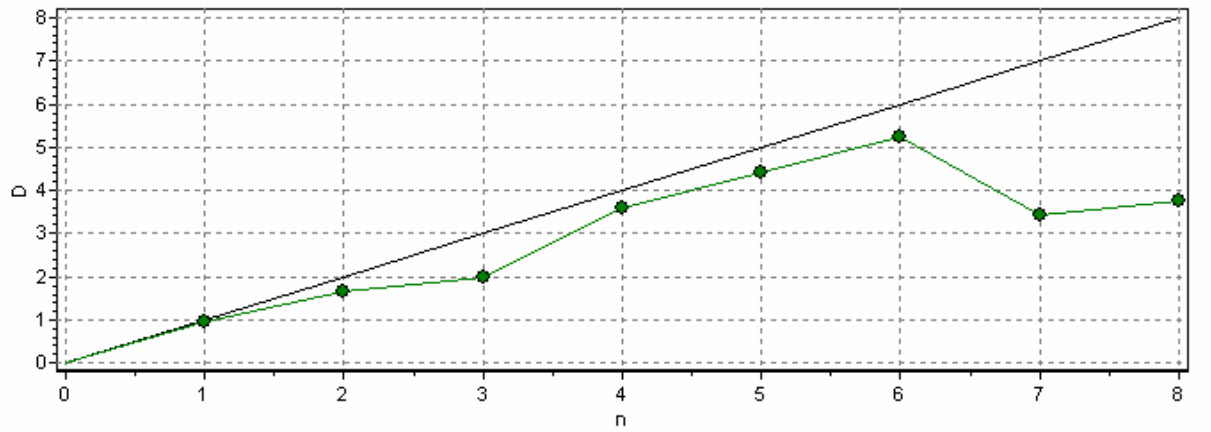

Figure 4.18. Correlation Dimension Graphic of Person-1 & State-1 (Application-2)

Correlation dimension D and embedded dimension n could be seen from Figure 4.18. Their measured values are 5,251 and 6. Correlation dimension value is quite high and looking at the autocorrelation function graphic (See Appendix C) the reason of being high dimensional could be understood.

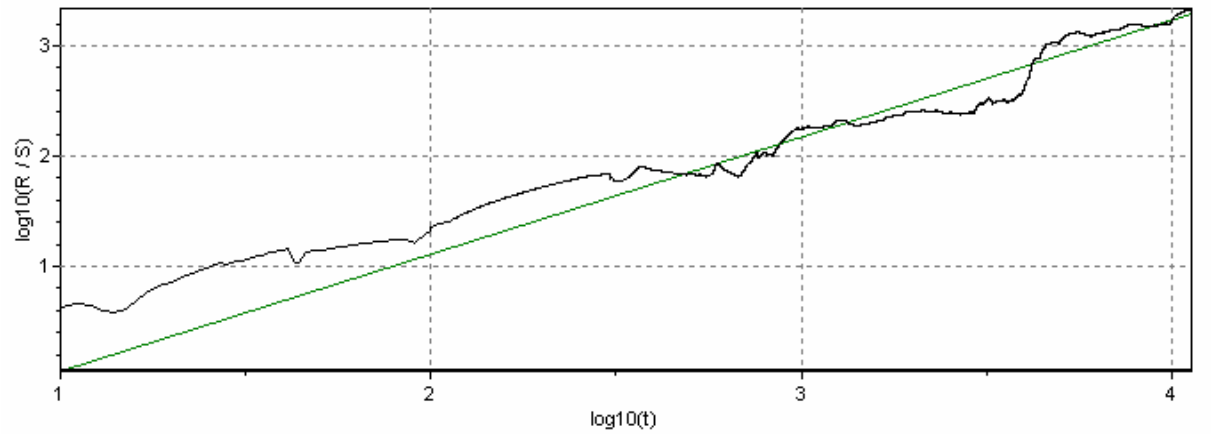

Figure 4.19. Hurst Exponent H and Hausdorff Dimension D of Person-1 & State-1 (Application-2)

Hurst exponent and Hausdorff dimension values were calculated according to ECG Signal of Person-1 & State-1 as it is demonstrated in Figure 4.19. Hausdorff Dimension value is 0,9388, where H equals to 1,0610.

4.2.3.2. Person-1 & State-2 (Walk)

- Sample size: 4789
- Sampling interval: 1/200 seconds
- X-axis: Time in seconds
- Y-axis: Amplitude in milivolts

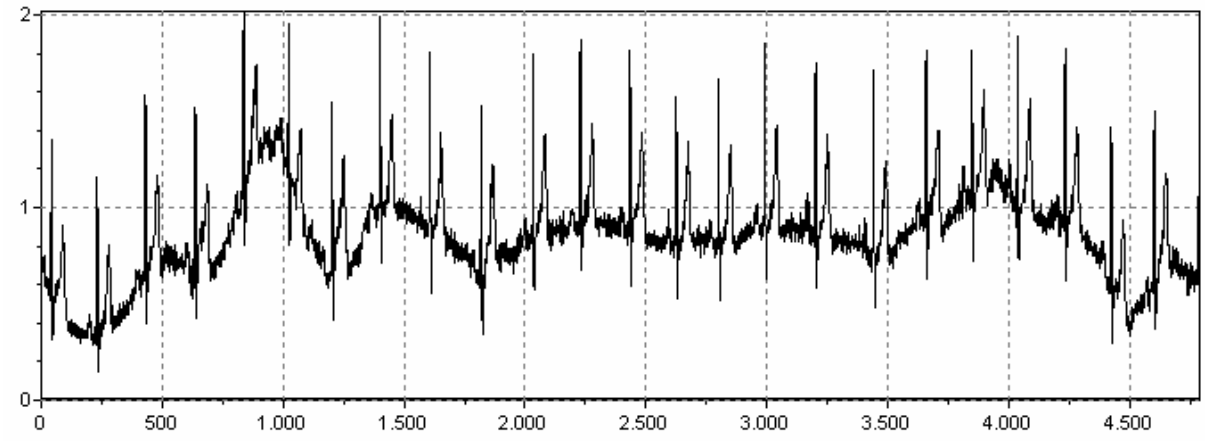

Figure 4.20. ECG Signal of Person-1 & State-2 (Application-2)

ECG Signal of Person-1 & State-2 tends to have partly undulation, shown in Figure 4.20. Because of movements of person-1 this undulation occured and therefore ECG signal looks not periodic.

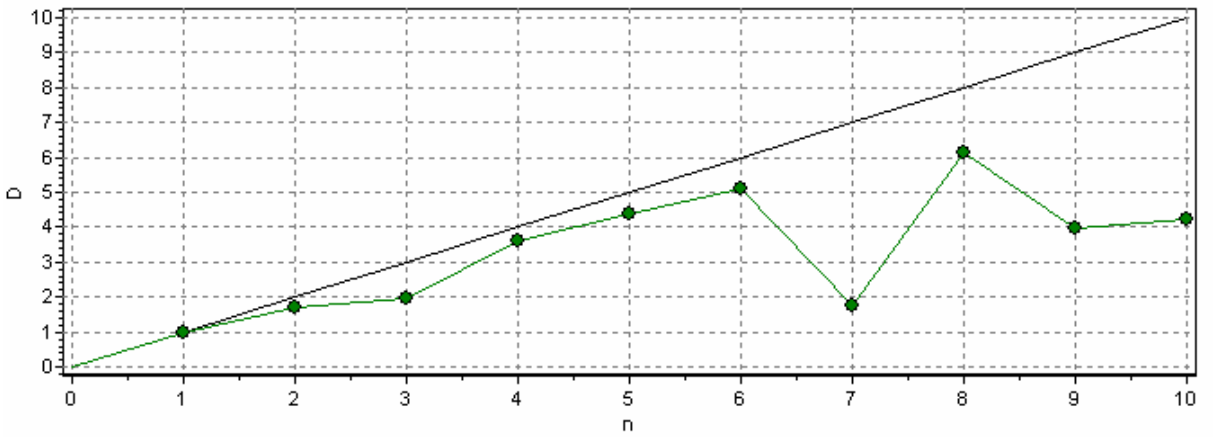

Figure 4.21. Correlation Dimension of Person-1 & State-2 (Application-2)

In this measurement correlation dimension value was quite high as it is recognized in Figure 4.21. It has the value of 6,148. In addition to this high dimension value, aotocorrelation values are also high, close to one.

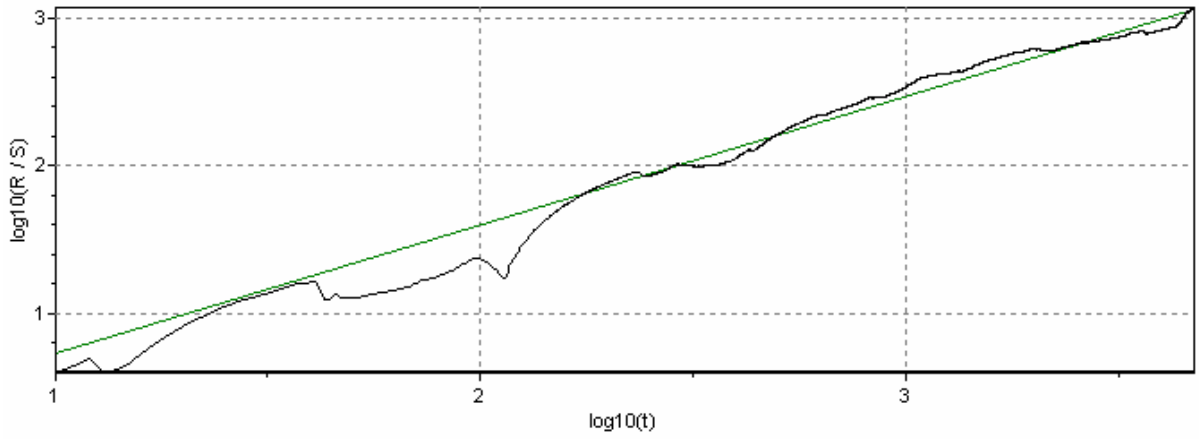

Figure 4.22. Hurst Exponent H and Hausdorff Dimension D of Person-1 & State-2 (Application-2)

In Figure 4.22. Hurst exponent graphic was demonstrated and according to calculations results values are; H = 0,8669 and D_H = 1,1331.

4.2.3.3. Person-1 & State-3 (Rapid walk)

- Sample size: 3000
- Sampling interval: 1/200 seconds
- X-axis: Time in seconds
- Y-axis: Amplitude in milivolts

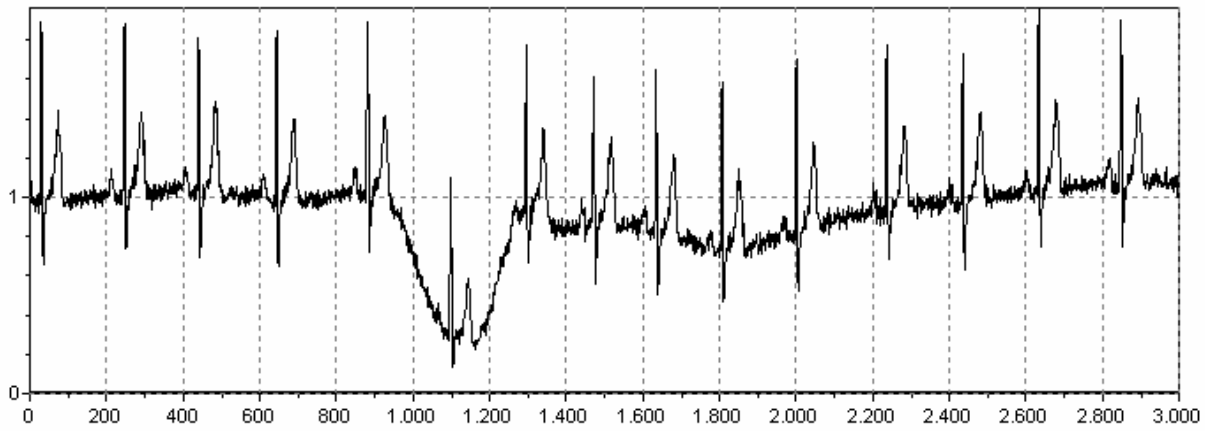

Figure 4.23. ECG Signal of Person-1 & State-3 (Application-2)

ECG Signal of Person-1 & State -3 in Figure 4.23. shows an abnormal behaviour between 1000 and 1200 samples. It can result from surroundings conditions or physiology of Person-1, because in the first application this behaviour did not occur in the same state.

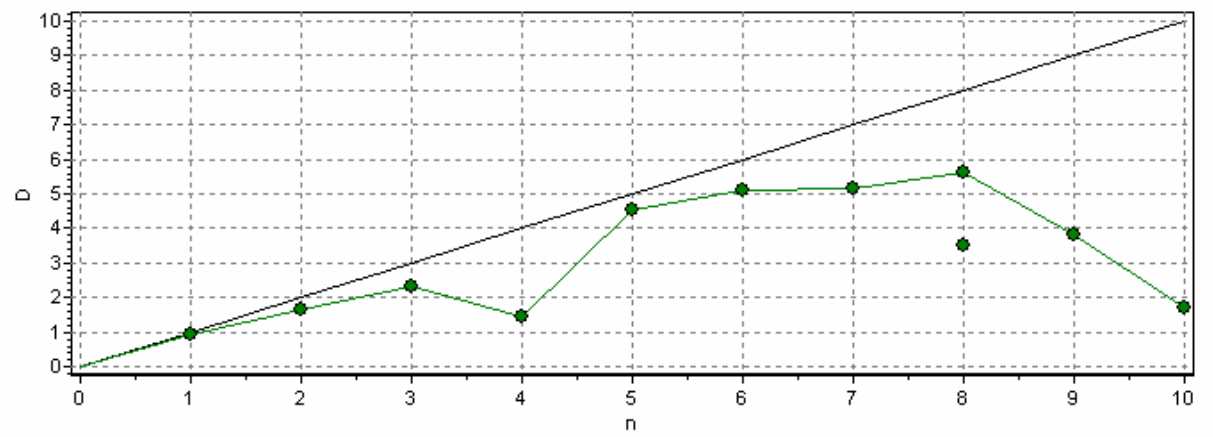

Figure 4.24. Correlation Dimension of Person-1 & State-3 (Application-2)

Correlation dimension value decreases again but does not reach at too low values and it is exhibited in Figure 4.24. Embedded dimension n has the value of 8, while correlation dimension D was taking the value of 5,627 and autocorrelation values never drop under 0, they are near 1.

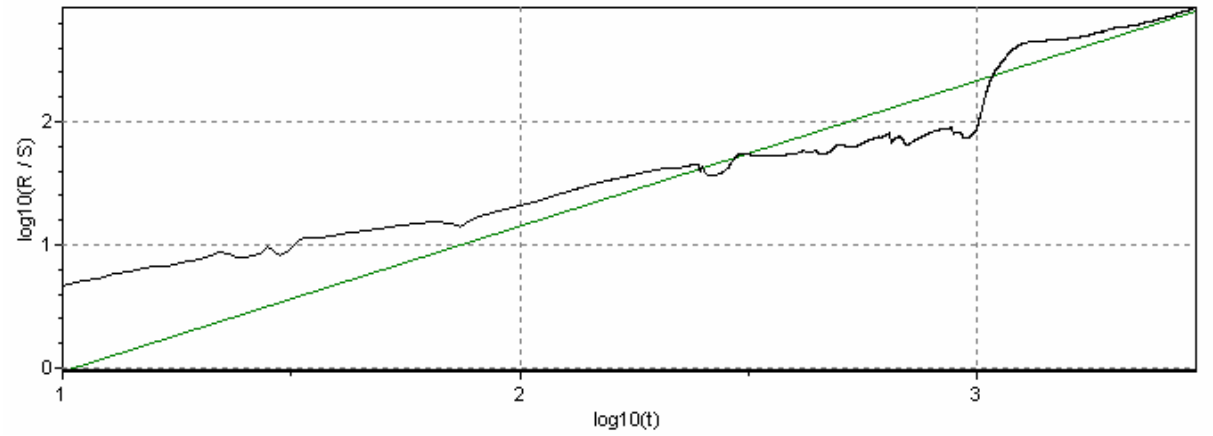

Figure 4.25. Hurst Exponent H and Hausdorff Dimension D of Person-1 & State-3 (Application-2)

H and D_H values were computed in Figure 4.25., taking the values H= 1,1846 and D_H = 0,8154. The Hausdorff dimension value decreases, concerning the two first states.

4.2.3.4. Person-1 & State-4 (Run)

- Sample size: 2004
- Sampling interval: 1/200 seconds
- X-axis: Time in seconds
- Y-axis: Amplitude in milivolts

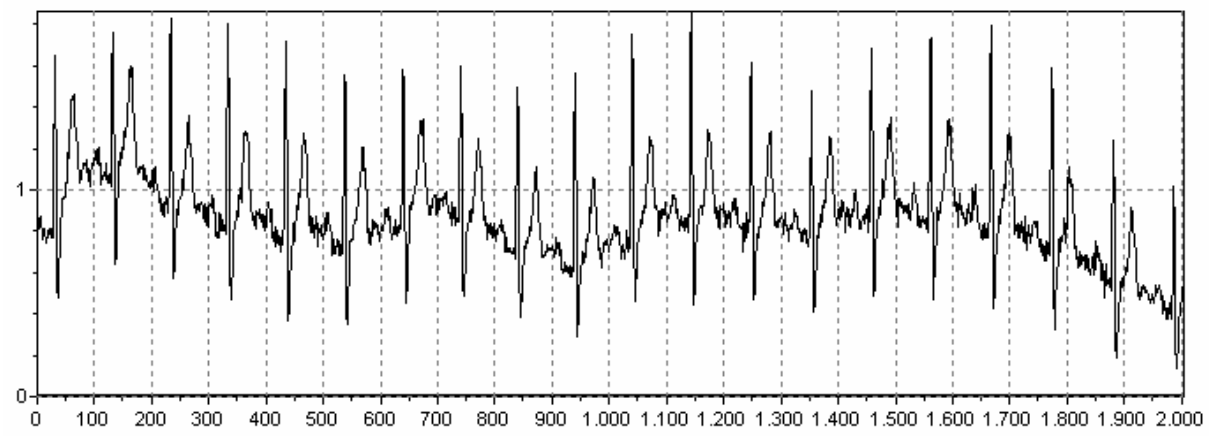

Figure 4.26. ECG Signal of Person-1 & State-4 (Application-2)

Although ECG Signal of Person-1 & State -4 was measured after run, this signal looks so regular that it seems like the signal in normal state. It shows a frequently periodic behaviour, given in Figure 4.26.

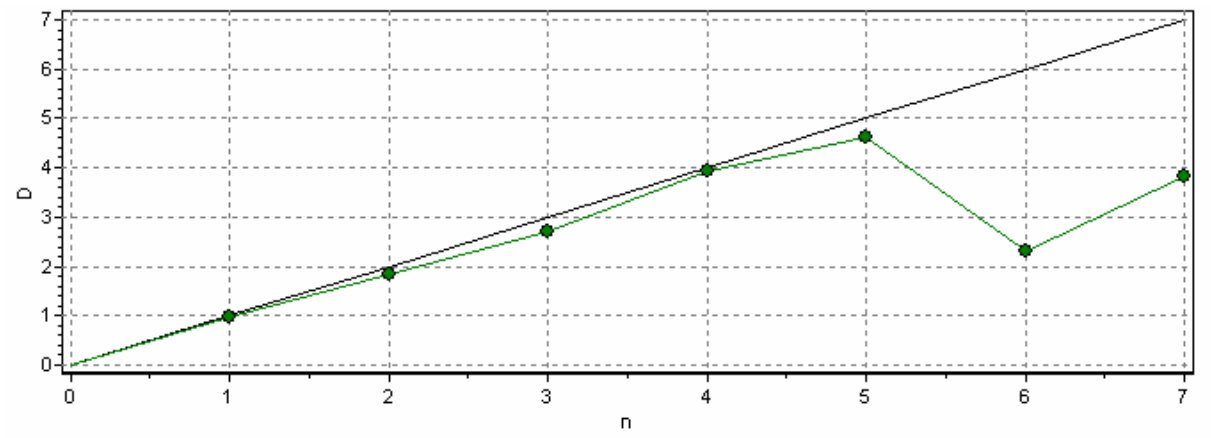

Figure 4.27. Correlation Dimension of Person-1 & State-4 (Application-2)

By way of finding the embedded dimension n at the value of 5, correlation dimension D was computed as 4,620, demonstrated in Figure 4.27. Correlation dimension value decreases, handling other three states. It could be also recognized from the autocorrelation function graphic, because rarely autocorrelation values drop under 0.

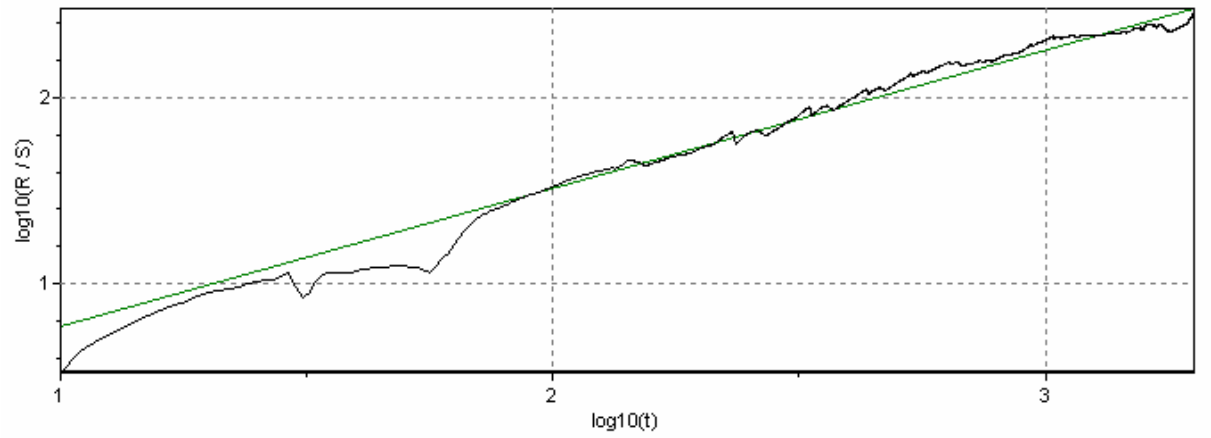

Figure 4.28. Hurst Exponent H and Hausdorff Dimension D of Person-1 & State-4 (Application-2)

Figure 4.28. shows the Hurst exponent H and Hausdorff dimension D_H of Person-1 & State-4 of Application-2, with values; H = 0,7437 and D_H = 1,2563.

4.2.4. Application-2 for Box-counting Dimension

4.2.4.1. Person-1 & State-1 (Normal)

Table 4.5. Calculated Box Sizes and Box Numbers of ECG Signal of Person-1 & State-1 (Application-2)

Box size	1	17	37	53	65	79	90	143	206	256
Box number	20816	277	76	43	31	22	19	9	6	6

Regression Equation

$\hat{y} = 9{,}86 - 1{,}520x$

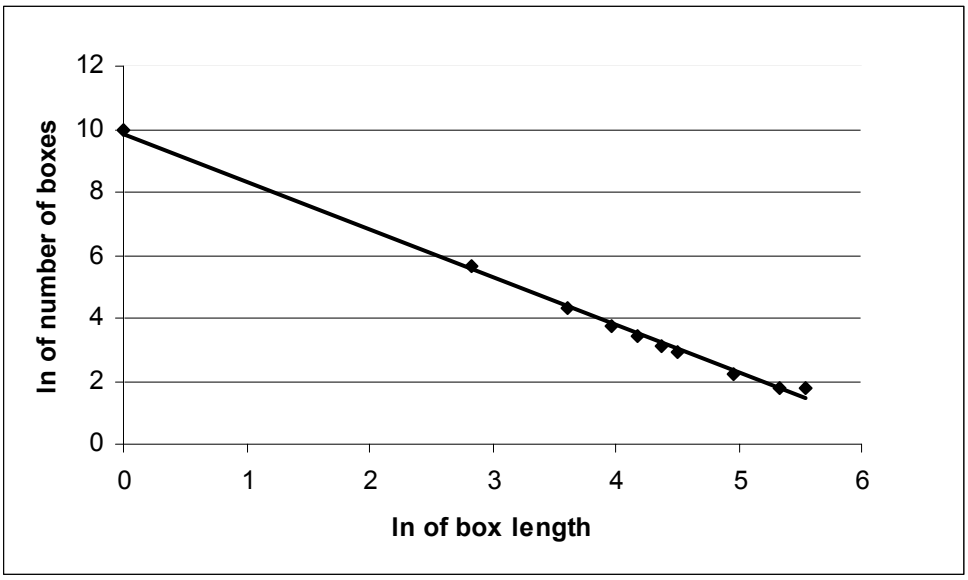

Figure 4.29. The Regression Line Graph of Person-1 & State-1 (Application-2)

4.2.4.2. Person-1 & State-2 (Walk)

Table 4.6. Calculated Box Sizes and Box Numbers of ECG Signal of Person-1 & State-2 (Application-2)

Box size	1	39	75	119	143	163	186	200	222	256
Box number	12804	63	27	12	9	8	6	6	6	4

Regression Equation

$\hat{y} = 9{,}46 - 1{,}449x$

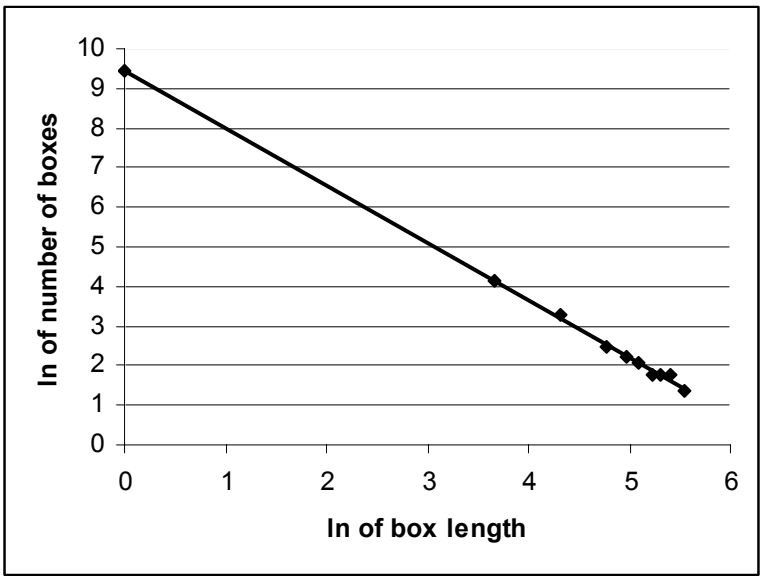

Figure 4.30. The Regression Line Graph of Person-1 & State-2 (Application-2)

4.2.4.3. Person-1 & State-3 (Rapid Walk)

Table 4.7. Calculated Box Sizes and Box Numbers of ECG Signal of Person-1 & State-3 (Application-2)

Box size	1	26	74	115	141	171	200	221	238	256
Box number	10585	140	29	12	9	7	6	6	5	4

Regression Equation

$\hat{y} = 9{,}35 - 1{,}423x$

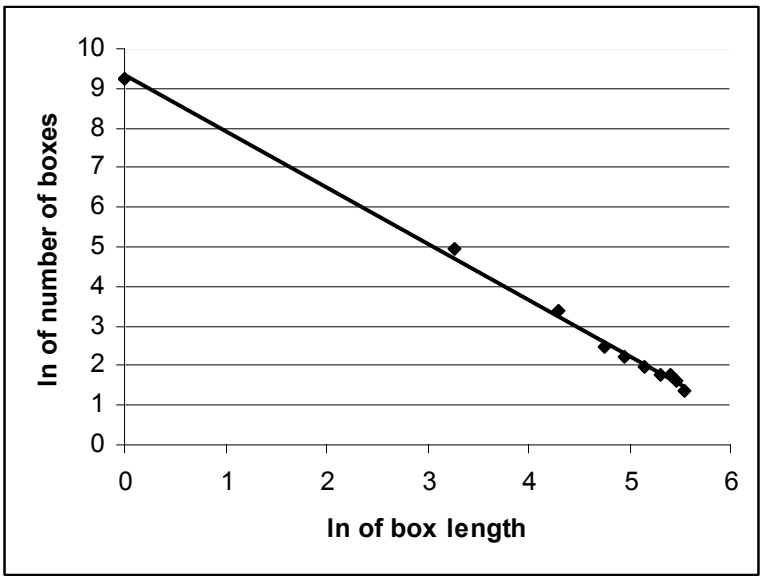

Figure 4.31. The Regression Line Graph of Person-1 & State-3 (Application-2)

4.2.4.4. Person-1 & State-4 (Run)

Table 4.8. Calculated Box Sizes and Box Numbers of ECG Signal of Person-1 & State-4 (Application-2)

Box size	1	32	68	105	146	173	196	214	231	256
Box number	12533	93	26	15	8	6	6	6	6	6

Regression Equation

$\hat{y} = 9{,}39 - 1{,}428x$

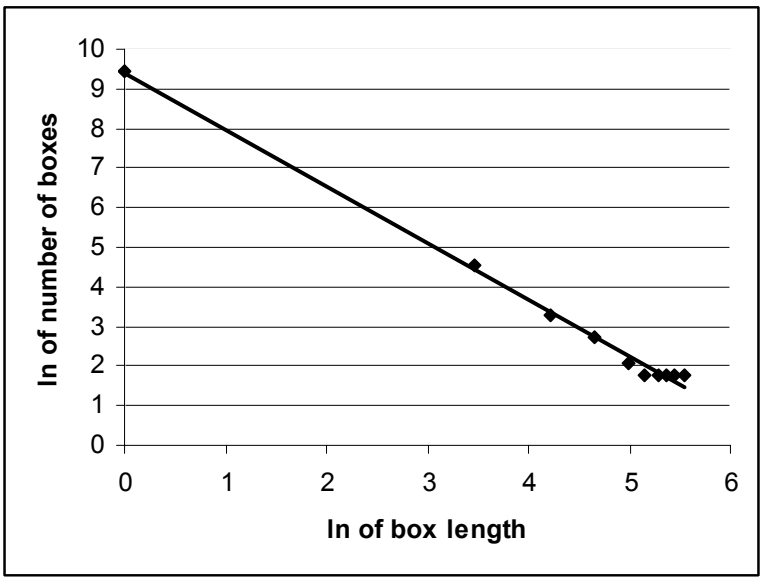

Figure 4.32. The Regression Line Graph of Person-1 & State-4 (Application-2)

4.3. Comparison of the Results

These dimension values of three persons in four states were exibited according to two applications. In application-1 the results were not consistent to each other. While some values were decreasing, some were increasing as it is seen in Table 4.9. This problem occurred not only depending on changing persons, but also handling the dimension kinds. Therefore another application was made through changing the sample size.

Table 4.9. Comparison of Three Fractal Dimensions for All Persons in Four States for Application-1

Person-1		Correlation Dimension	Hausdorff Dimension	Box-counting Dimension
	State-1	3,462	1,275	1,36
	State-2	4,031	0,951	1,26
	State-3	3,863	1,382	1,29
	State-4	2,373	1,155	1,39
Person-2				
	State-1	6,831	1,606	1,37
	State-2	5,125	1,641	1,40
	State-3	6,170	1,416	1,42
	State-4	6,243	0,978	1,42
Person-3				
	State-1	3,698	1,535	1,33
	State-2	3,313	0,894	1,27
	State-3	2,788	1,027	1,29
	State-4	3,365	1,443	1,38

As it is demonstrated below in table 4.10., new obtained values were more consistent than the earlier. Almost all values, concerning the dimension classification were catching the harmony. In order to recognize the harmonic trend it is obvious to plot the variation analysis graphs, because from numerical values it is difficult to see it clearly. On the other hand these results provide making decision about that the dimension values do not decrease or increase related to the changing states proportionally.

Table 4.10. Comparison of Three Fractal Dimensions for All Persons in Four States for Application-2

Person-1		Correlation Dimension	Hausdorff Dimension	Box-counting Dimension
	State-1	5,25	0,93	1,52
	State-2	6,14	1,13	1,44
	State-3	5,62	0,81	1,42
	State-4	4,62	1,25	1,42
Person-2				
	State-1	6,79	1,46	1,45
	State-2	8,06	1,38	1,57
	State-3	7,40	1,08	1,58
	State-4	6,21	1,35	1,57
Person-3				
	State-1	4,40	1,47	1,42
	State-2	5,46	1,27	1,46
	State-3	5,04	0,82	1,38
	State-4	4,17	1,29	1,43

4.4. Dimension vs. States Analysis of Application-1

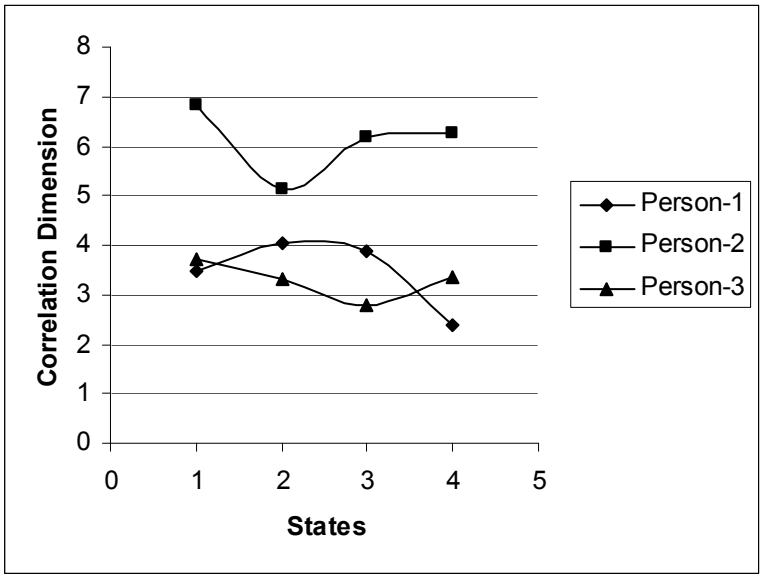

Figure 4.33. Correlation Dimension vs. States Graph of Three Persons for Application-1

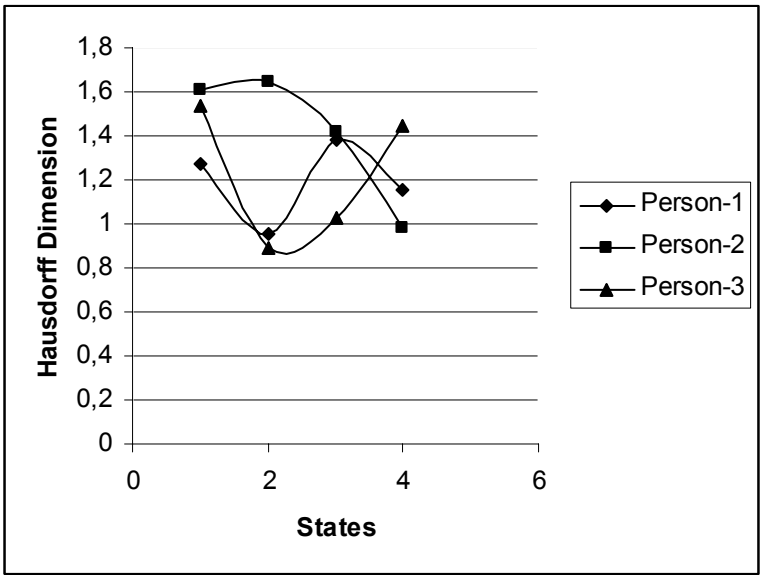

Figure 4.34. Hausdorff Dimension vs. States Graph of Three Persons for Application-1

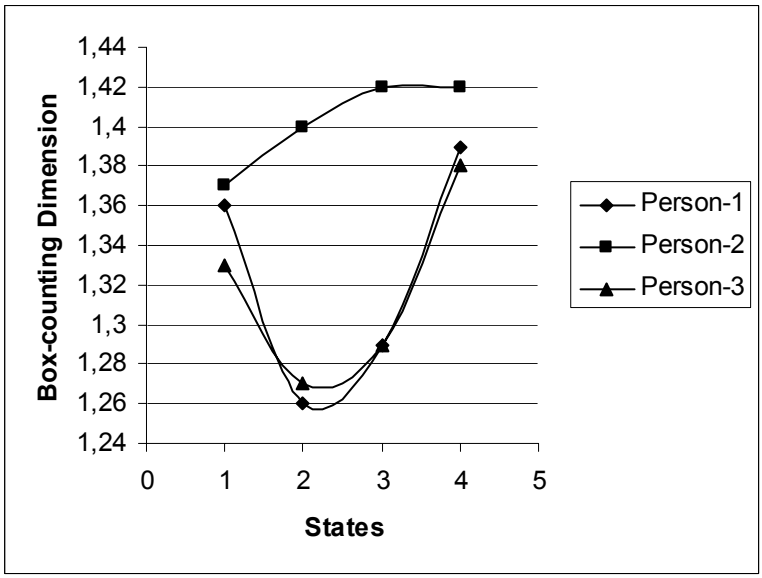

Figure 4.35. Box-counting Dimension vs. States Graph of Three Persons for Application-1

4.4.1. Comparison of Dimension vs. States Analysis Results of Application-1

According to dimension vs. states analysis graphs of application-1, as it was mentioned in comparison of numerical results, there was a disharmony between measured values. Dimension vs. states analysis graph of correlation dimension shows this disharmony in a good manner in Figure 4.33. Anyway it was not expected that the measured data were highly carrelated in eachother, concerning the correlation function graphs, because almost in all states correlation function values reached at the value zero, which means that the correlation is weak there. However person-2 shows a good correlation and it can be understood also from numerical results, because measured values are quite high. Persons' Hausdorff dimension values are not harmonic seing the paths in figure 4.34. It means that Hausdorff dimension measurements did not give any reasonable result. On the other hand box-counting dimension values of person-1 and person-3 reach at the consistence in second, third and fourth states, as it is seen in Figure 4.35. According to this demonstration it is obvious that box-counting dimension gives more accurate results rather than Hausdorff dimension.

4.5. Dimension vs. States Analysis of Application-2

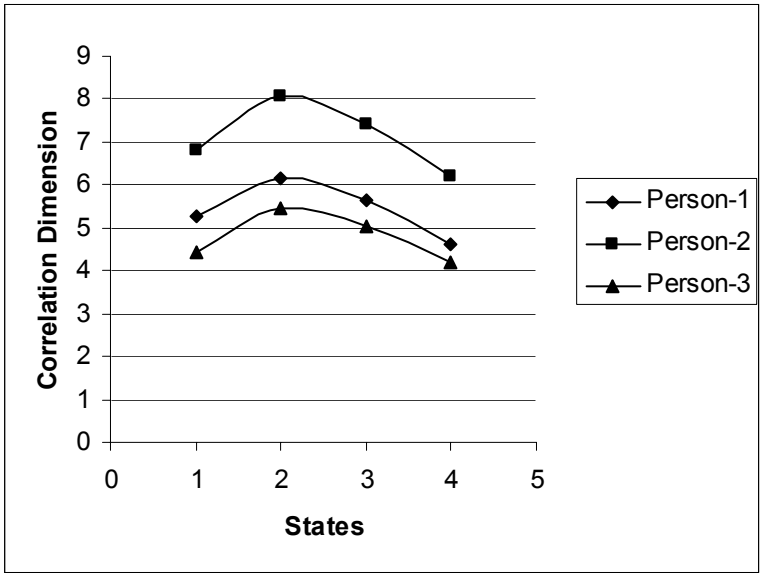

Figure 4.36. Correlation Dimension vs. States Graph of Three Persons for Application-2

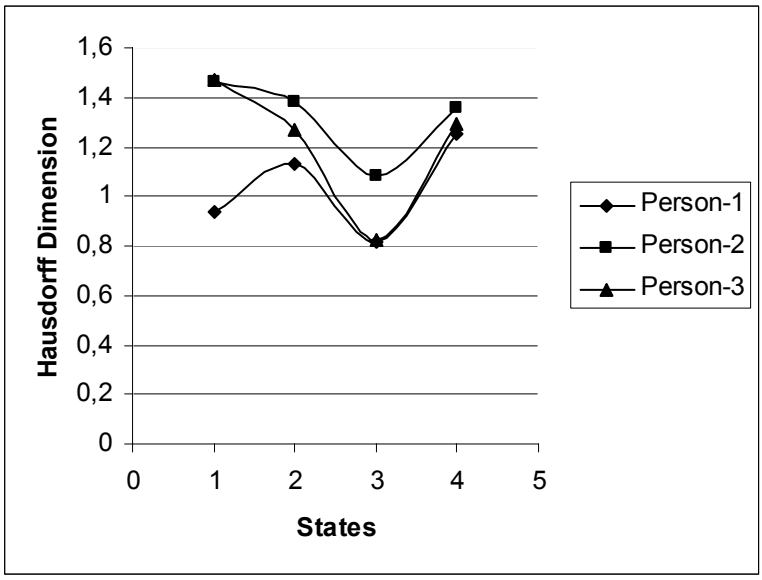

Figure 4.37. Hausdorff Dimension vs. States Graph of Three Persons for Application-2

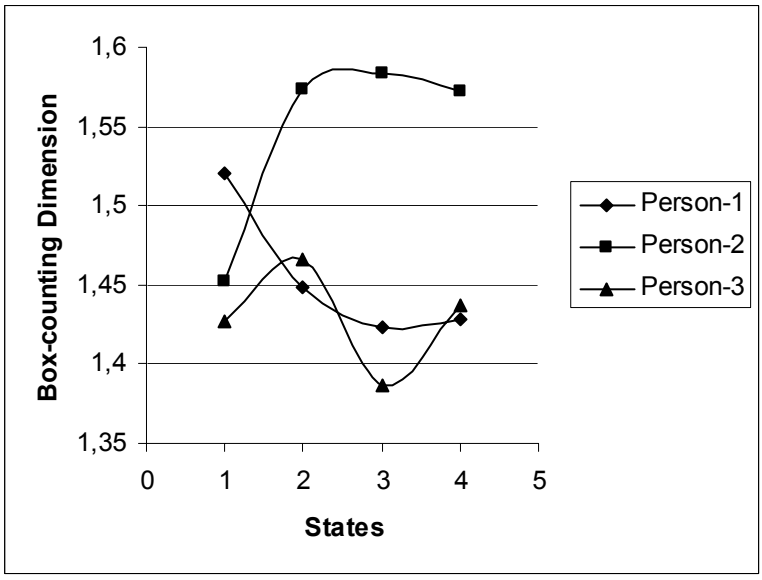

Figure 4.38. Box-counting Dimension vs. States Graph of Three Persons for Application-2

4.5.1. Comparison of Dimension vs. States Analysis of Application-2

According to this application the balance of the harmony between persons changes in all dimension types. Looking at Figure 4.36. correlation dimension measurements catch the consistency, all paths were arranged in a parallel manner. It is also the scale of that the data points are highly correlated and correlation function value is nearly one in four states. Again person-2 has the most correlation. In this application Hausdorff dimension measurements seem more consistent than the box-counting measurements. These values reach consistency in the second state and this consistence remains until the end of the measurement, as it is seen in the Figure 4.37. On the other hand contrast to first application box-counting dimension values create strange structures in Figure 4.38., which are not consequential.

CHAPTER 5

CONCLUSIONS

This thesis has probed into detection and diagnosis through examining ECG signals of three distinct persons in different four states. These signals were inspected according to three dimension calculation methods, correlation, Hausdorff and box-counting dimensions. In calculating correlation dimension, autocorrelation function provided assistance and also its graphs were used to see how correlated are the data with each other. On the other hand, because of the difficulty with the computation of the Hausdorff dimension, the Hurst exponent was utilized in finding the Hausdorff dimension values. During calculation of box-counting dimension data, box-sizes and box-numbers were obtained automatically via a software package, but there was the need for calculation of regression equation, because the slope of the regression line gives the box-counting dimension. All these correlation, Hausdorff and box-counting dimension calculations were made twice and grouped into two, named application-1 and application-2.

These applications differ according to sample size. In the first application 1000 data were chosen, whereas in the second application the whole set was taken. The classification was not restricted to only two groupings. Measurements and comparisons also were sorted according to the persons and dimensions. They were shown as well as graphical comparisons, such as tables, demostrating measured dimension values. After comparison of the results, it was noticed that fractal dimension all by itself is not adequate to make certain decisions about the system performance, because fractal dimension values do not range always systematically. Occasionally, some dimension method calculation results show independence with each other, whereas others appear with harmonious results. At the beginning of this thesis, it was expected that the fractal dimension values will be almost the same, because the formula of these methods are alike, concerning the power law behaviour. Because any minor change in the signal, varies the complete fractal dimension value, therefore it can be also expressed as a disadvantage utilizing these methods.

In addition to this disadvantage, according to the results, it is recognized that dimension values do not proportionally decrease or increase related to the changing states. It may very well be due to the fact that the number of people involved in the experiments is not sufficient to further prove any point. Experiments were done for three persons in distinct four states. If this experiment had been applied for more persons, the results could have been consistent with the states.

It is recognized that the Hausdorff dimension calculation seems to give the best result among the used methods because it covers the whole set. This characteristic of the coverage results from covering the set using balls of different diameters, instead of using coverings of the same size as in the box-counting method. Therefore, it could be commented that the box-counting method has some disadvantages at accurate dimension calculation of an image. Using boxes of the same size means that the coverage has some lacunas there, each box can not occupy any part of the image of the same size (Definition and calculation of Lacunarity were expressed in Appendix B). Counting all boxes as the same quality, results in some calculation errors. In other words, it can also be expressed as counting money without caring about the banknote values.

As for the correlation dimension values, it is obvious that the results are quite high in values, in handling the result of a sinusoidal wave. But it could be also useful in order to see the correlation between data points. Hausdorff and box-counting dimension values are alike in some states but correlation dimension values differ. On the other hand it is also possible that correlation dimension has its own range in the boundaries of fractal dimension.

Altough these kinds of fractal dimension methods have some disadvantages, this approach is a way to compare time series under changing work conditions, concerning the machinery, especially material science. In this thesis ECG signals were used to show that this method is universal. Taking fractal dimension measurements from many healthy specimens may bring a range, called healthy fractal range, in order to separate the faulty set.

REFERENCES

Barnsley, M. F., 1993. "Fractals Everywhere" (AP PROFESSIONAL, Boston, San Diego, New York, London, Sydney, Tokyo, Toronto), Second Edition.

Barnsley, M. F., Demko, S., 1985. "Iterated Function Systems and the Global Construction of Fractals", The *Proceedings of the Royal Society of London* A399: 243-275.

Barnsley, M. F., 1986. "Fractal Functions and Interpolation", *Constructive Approximation* 2: 303-329.

Butterfield, J.I., 1991. "Fractal Interpolation of Radar Signatures for Detecting Stationary Targets in Ground Clutter", *Georgia Tech Research Institute, Georgia Institute of Technology*, Atlanta, GA 30332, 10.1109/NTC.1991.147991.

Curry, J., Garnett, L., Sullivan, D.,1983. "On the Iteration of Rational Functions: Computer Experiments with Newton's Method", *Communications in Mathematical Physics* 91: 267-277.

Dieker T. 2004 "Simulation of Fractional Brownian Motion", *University of Twente Department of Mathematical Sciences, The Netherlands.*

Dublin, D., 2000. "Rapid Interpretation of ECG's, (Cover Publishing).

Falconer, K., 1990. "Fractal Geometry", *University of Bristol* edited by J. Wiley & Sons Ltd. Baffins Lane, Chichester West Sussex PO19 1 UD, England.

Federer, H., 1969. "Geometric Measure Theory". Springer-Verlag, New York.

Gilbert, W. J., 1982. "Fractal Geometry Derived from Complex Bases", *The Mathematical Intelligencer* 4: 78-86.

Hasfjord F. 2004 "Heart Sound Analysis with Time Dependent Fractal Dimensions", *Department of Biomedical Engineering at Linköpings university* LiU-IMT-EX-358 2004-02-25.

Hata, M., 1985. "On the Structure of Self –Similar Sets", *Japan Journal of Applied Mathematics* 2(2): 381-414.

Hutchinson, J., 1981. "Fractals and Self-Similarity", *Indiana University Journal of Mathematics* 30: 713-747.

İkiz F., Püskülcü H., Eren Ş., 2000. "Istatistiğe Giriş", (Fakülteler Kitabevi Barış Yayınları, Izmir), ISBN-975-94951-0-4.

Leung, D., Romagnoli, J. 2000. "Dynamic probabilistic model-based expert system for fault diagnosis", *Computers and Chemical Engineering,* 24 (2000) 2473-2492.

Marques de Sá, J.P. 1999. "Fractals in Physiology", *A Biomedical Engineering Perspective.*

Miksovsky J., Raidl A. 2001 "On some nonlinear method of meteorogical time series analysis", WDS 2001 conference (Week of doctoral students, Charles University).

Purkait, P., Chakravorti S. 2003. "Impulse Fault Classification in Transformers by Fractal Anlysis" *IEEE Trans. on Dielectr. and Electr. Insul.* Vol. 10, No.1, February, pp 109-116.

Ringler, A. T., Roth A. P. 2002. "Properties of the Correlation Dimension of Bounded Sets", *Pennsylvania State University Summer Mathematics* REU.

Scheffer, R., Filho, R. M. 2001 "The Fractional Brownian Motion as a Model for an Industrial Airlift Reactor" *Chemical Engineering Science* Vol:56, Issue:2, pp. 707-711.

So, P., Barreto, E., Hunt, B. R. 1999. "Box-counting dimension without boxes: Computing D_0 from average expansion rates", *in Physical Review* E 60 #1, p. 378-385.

Tang, Y. Y., Tao, Y., Lam, C.M..E. 2002. "New Method for Feature Extraction Based on Fractal Behaviour" PR(35), No:5, www Version.0202 BibRef.

Web_1, 1998. Fractals, 15/02/2005. http://www.home.inreach.com/kfarrell/fractals.html

Web_2, 1993. Spread Spectrum: Voice Link Over Spread Spectrum Radio, 28/03/2005 "Auto-Correlation and Cross Correlation", http://www.tapr.org/ss_g1pvz.html#correlation.

Wu, J. D., Huang, C. W., Huang, R. 2004 "An application of a recursive Kalman filtering algorithm in rotating machinery fault diagnosis", NDT&E International xx (2004) xxx-xx

APPENDIX A

FRACTAL GEOMETRY DEFINITIONS

R ^{n} : n – dimensional Euclidean Space. (R^2 = Euclidean plane)

E, F, U : Sets, which will generally be subsets of R^n

E $\subset$ **F** : E is a subset of the set F

x $\subset$ **E** : The point x belongs to the set E

{x:condition} : The set of x for which "condition" is true

Z : Integers (Z^+ : Positive integers)

Q : Rational Numbers

R $^+$: Positive Real Numbers

C : Complex Numbers

B $_r$ **(x)** = $\{y : | y - x | \leq r\}$: The closed ball of center x and radius r

B ^0_r **(x)** = $\{y : | y - x | < r\}$:The open ball

Closed ball : Closed ball contains its bounding sphere

Open ball : Does not contain. In R^2, a ball is a disc, in R^1, a ball is just an interval

{x : a≤x≤b} for a<b, [a,b] : Closed interval

{x : a<x<b} for a<b, (a,b) : Open interval

{x : a≤x<b} for a<b, [a,b) : Half - open interval

Coordinate Cube of side 2r, center x = $(x_1,..., x_n)$

$\{y = (y_1,..., y_n) : | y_i - x_i | \leq r$ for i = 1, ... , n$\}$

A cube in R^2 is a square and in R^1 is an interval

δ – Parallel Body : A_δ, of a set A, that is the set of points within distance δ of A thus

$A_\delta = \{x : | x - y | \leq \delta$ for some y in A$\}$

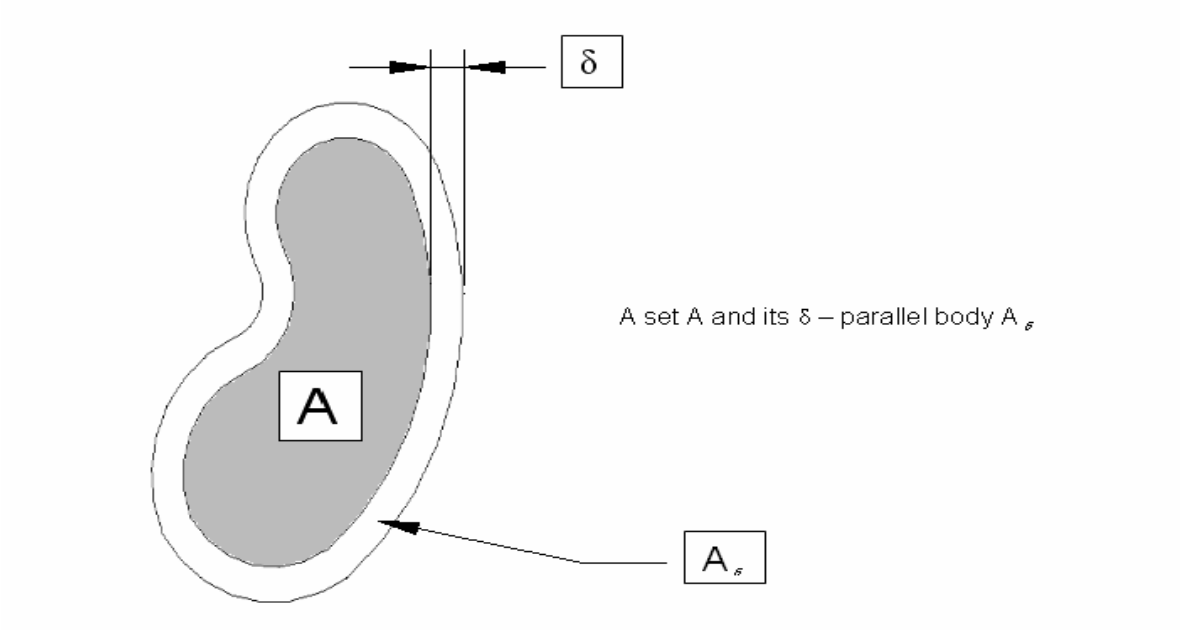

Figure A.1. A set A and its δ-parallel body A_δ

Disjoint Sets : $A \cup B = \emptyset$

A\B , The Difference : Consists of points in A but not B

The Compliment of A : $IR^n \backslash A$

Product of A&B : Cartesian Product, denoted by AXB. If $A \subset IR^n$ and $B \subset IR^m$ then $AXB \subset IR^{n+m}$

Countable Sets : Infinite set A is countable if its elements can be listed in the form x_1, x_2 ...with every element of A appearing at a specific place in the list . The sets Z and Q are countable but IR is uncountable.

Supremum sup A : A being any set of real numbers , sup A is the least number m such that $x \leq m$ for every x in A, or sup A is ∞ if no such number exists.

Infimum inf A : is the greatest number m such that $m \leq x$ for all x in A , or inf A = $-\infty$.

Intuitively, supremum and infimum are thought of as the maximum and minimum of the set A itself.

$\mathrm{Sup}_{x\in B}$ (A) : Supremum of A , which may depend on x, as x ranges over the set B .

Diameter $|A|$: The greatest distance apart of pairs of points in A .Thus

$|A| = \sup\{|x-y| : x,y \in A\}$.

Bounded Set : A set is bounded if it has finite diameter .

Open and Closed Sets : A set is open if and only if its complement is closed . The union of any collection of open sets is open, as is the case in intersection .The same goes for the closed sets .

Closure of A , $\overline{A}$: The intersection of all the closed sets containing a set A .

Interior of A , int(A) : The union of all the open sets contained in A . The cosure of A is thought of as the smallest closed set containing A , and the interior as the largest open set contained in A .

Boundary ∂A of A : $\partial A = \overline{A} \setminus \mathrm{int}(A)$

Dense Subset : A set B is a dense subset of A if $B \subset A \subset \overline{B}$, i.e. if there are points of B arbitrarily close to each point of A .

Compact Set : A set is compact if any collection of open sets which covers A (i.e. with union containing A) has a finite sub collection which also covers A .It is enough to think of a compact sub set of IR^n as one that is both closed and bounded .

Connected Sets : A subset A of IR^n is connected if there do not exist open sets U and V such that $U \cup V$ contains A with $A \cap U$ and $A \cap V$ disjoint and non-empty . Intuitively , we think of a set A as connected if it consists of just one “piece” . The largest connected subset of A containing a point x is called the “connected component of x “.

Totally Disconnected Sets : The connected component of each point consists of just that point.

Borel Sets : Borel sets are the smallest collection of subsets of IR^n with the following properties :

- Every open set and every closed set is a borel set .
- The union of every finite or countable collection of borel sets is a Borel set , and the intersection of every finite or countable collection of Borel sets is a Borel set .

Roughness presents everywhere and helps to illustate why mathematical fractals are of extensive applicable pertinence and why fractal geometry is not about to activate of fuzzy challenges .

Fractal geometry has an independent life in a way of its own and it can be introduced as a "virtual discipline" in other words one cannot belive that fractal geometry as a "regular" discipline . One could express fractal geometry by describing its methds of operation as an creative "method" .

Once more , fractal geometry has one center in mathematics and in varied discoveries that scale-invariant roughness exist everywhere (both natural and synthetic structures) but can be treated quantitatively , if fractality will not be describe as an already almost banal form of structure .

A scale-invariant roughness recognition is necessary to perform in two parallel and mutually area : These are new tools of statistics and data analysis and use of those tools if they are proper , beyond the boundaries of ordinary disciplines .

The original fractal toolbox was begun with accomodated versions of down-to earth findings and mathematicall tools . Historically , the first was the "power law" probability distribution $Pr\{U>u\}\sim u^{\alpha}$, for which α is a critical exponent . This distribution had largely stayed on the margins of statistics, "(Federer 1969)".

APPENDIX B

LACUNARITY

The fractal dimension takes a consequential position among the several features of fractals . As a problem , just measuring the fractal dimension is not enough when the fractal dimension do not be powered with any other information , it can cause an impact that two differently appearing surfaces with the same value of "D" could not be seperated from each other . Except quantitativ dimension and emptiness measurement , one needs another criterium , fractal lacunarity . Topological and dimensional identical fractals may "look" very different . The holes or "lacunas" that are a obvious characteristic of fractality may be different in each situation . In this way , the term called lacunarity "Λ" was put in use by Mandelbrot, which can express the quantity of an image . The usage of lacunarity provides the determination of gaps or lacuna in the pattern . We can declare this term as it is shown below ;

$$\Lambda = E[(M/E(M))-1]^2 \qquad \text{(B.1)}$$

where "M" is the mass of the fractal set, and "E(M)" is the expected mass. The mass "M" of a fractal set is dependent on the lenght "L" of the measuring device-governed by the power law

$$M(L) = KL^{D} \qquad \text{(B.2)}$$

Where "K" is a constant. The lacunarity, thus, is a function of "L". Let "P(m,L)" be the possibility that there are"m" points within a box of side "L". Then "P(m,L)" is normalized, as below for all "L"

$$\sum_{m=1}^{N} P(m,L) = 1 \qquad \text{(B.3)}$$

where “N” is the number of possible points within the box. Let the total number of points in the images is “M”. Then the number of boxes with “m” points inside the box is “(M/m)P(m,L)”. $\Lambda(L) = [M^2(L) - [M(L)]^2] / [M(L)]^2$ This formula can be extracted as lacunarity, “(Purkait and Chakravorti 2003)” .

Anyway , apart this comparison role , lacunarity has a different potential , should discuss it . Actually , in early years , fractals were believed as mental pictures of how they look like . Concerning the shape of fractals or how look they , a lot of scientists surprised which tools to use to seek confirmation of fractality and determine further study . Unfortunatelly there was a big problem , only looking at fractals did not work , because low-lacunarity fractals can look nonfractal , so scientists could be leaded to be mis-identified . It is not the aim to build a list of natural fractals , whereas the main concern is that anonymous fractals are studied with unsuitable tools , and they potentially lead to confusion , instead of assisting .

APPENDIX C

AUTOCORRELATION FUNCTION GRAPHS

In this Appendix autocorrelation graphs of Person-1 in four states were given according to two applications. In graphs, on the x axis s represents the time lag in milliseconds and on the y axis B represents the correlation between data points.

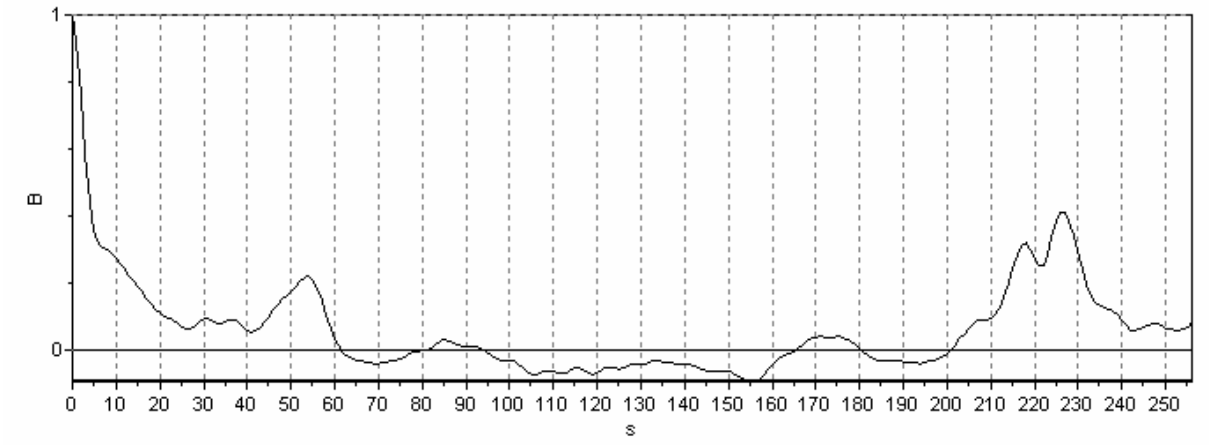

Figure C.1. Autocorrelation Function Graphic of Person-1 & State-1 (Application-1)

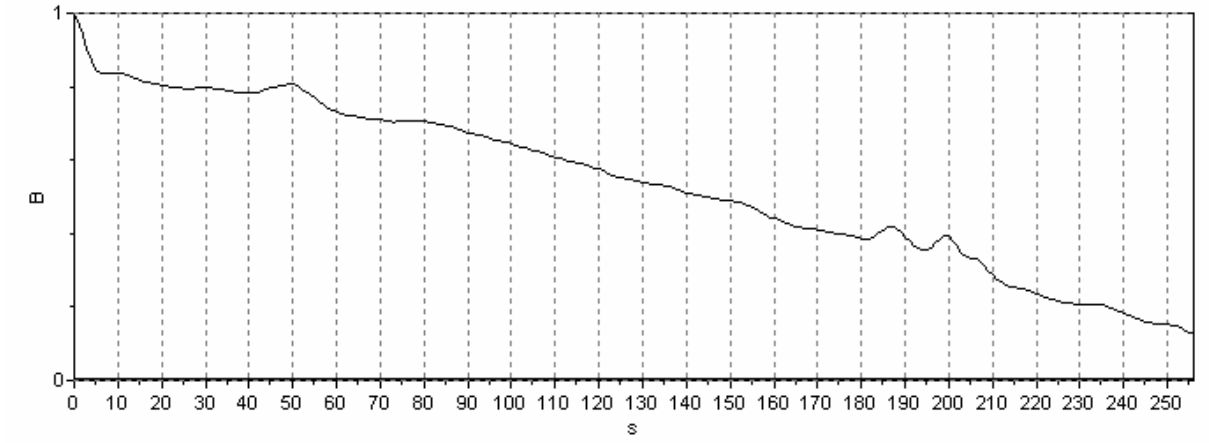

Figure C.2. Autocorrelation Function Graphic of Person-1 & State-2 (Application-1)

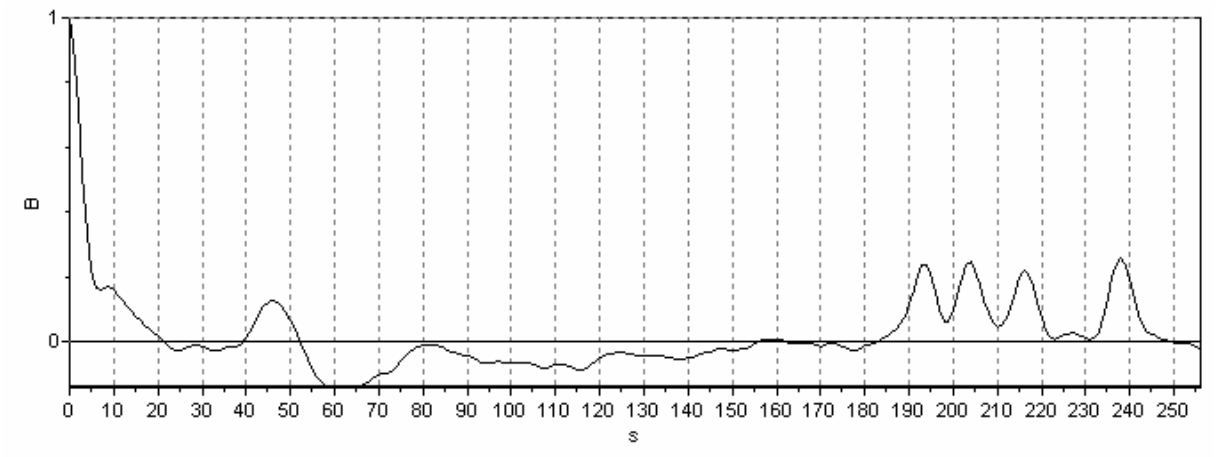

Figure C.3. Autocorrelation Function Graphic of Person-1 & State-3 (Application-1)

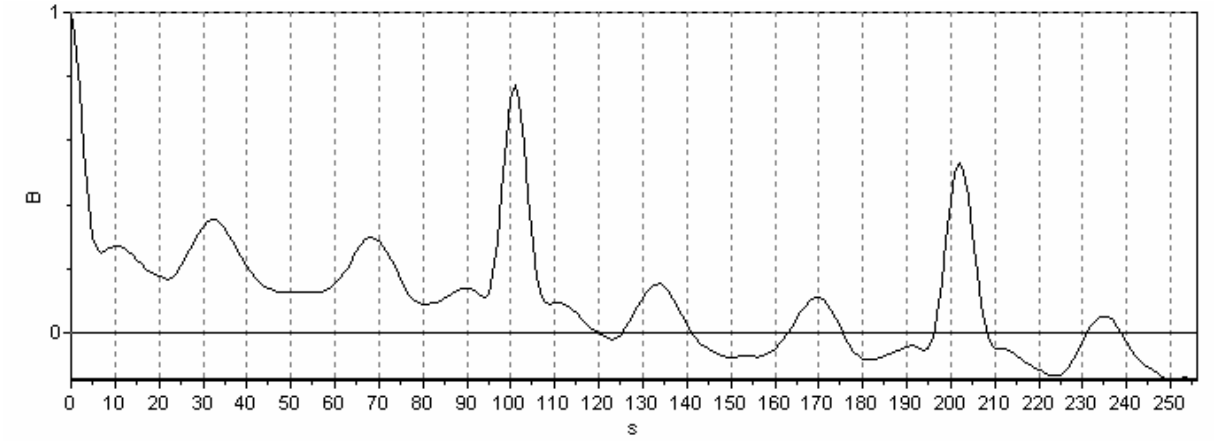

Figure C.4. Autocorrelation Function Graphic of Person-1 & State-4 (Application-1)

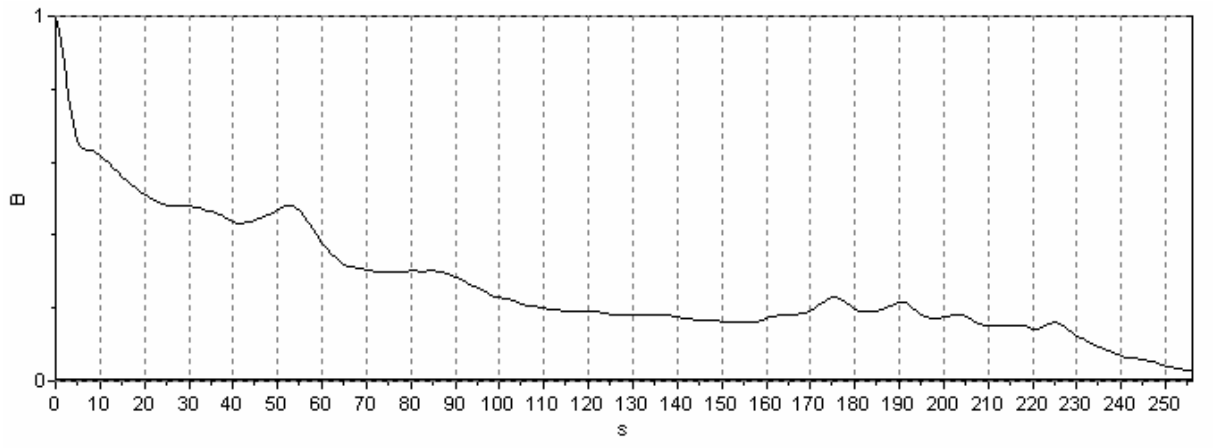

Figure C.5. Autocorrelation Function Graphic of Person-1 & State-1 (Application-2)

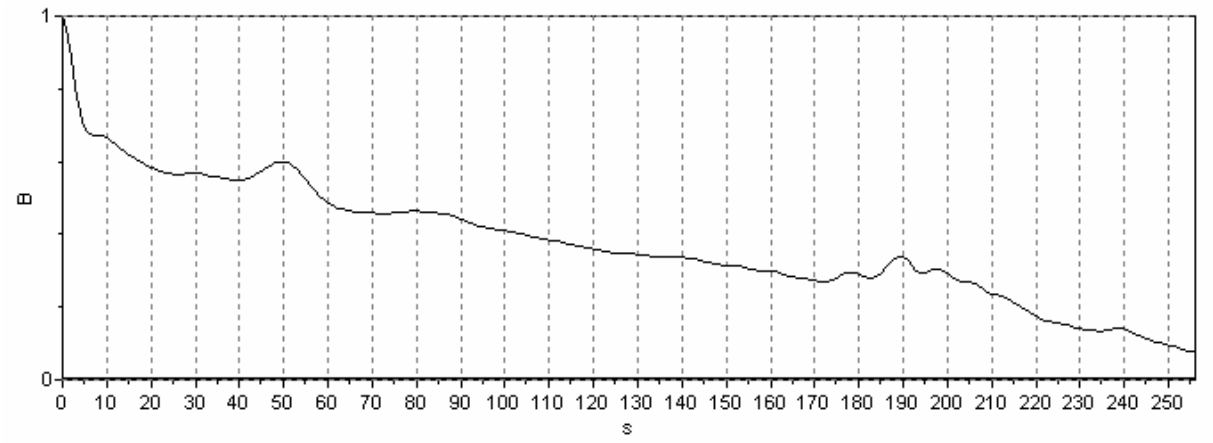

Figure C.6. Autocorrelation Function Graphic of Person-1 & State-2 (Application-2)

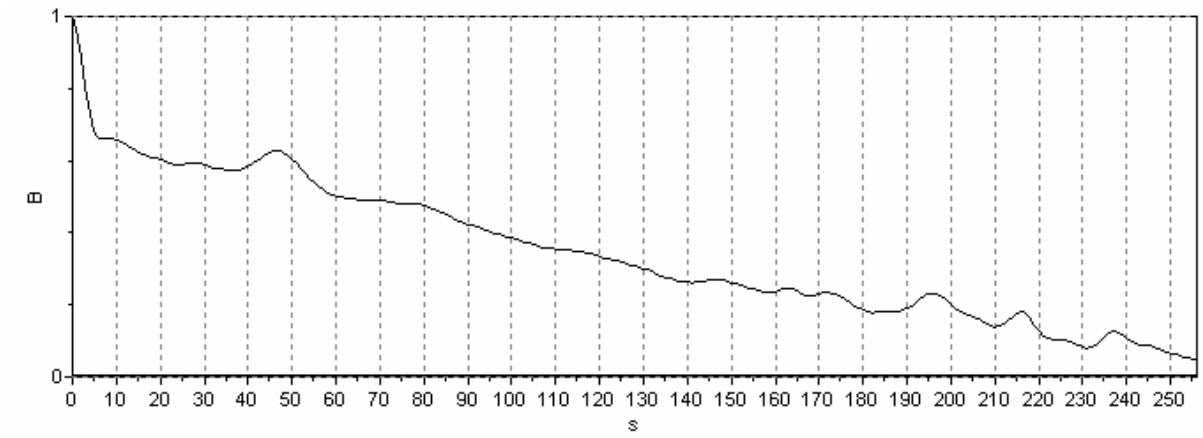

Figure C.7. Autocorrelation Function Graphic of Person-1 & State-3 (Application-2)

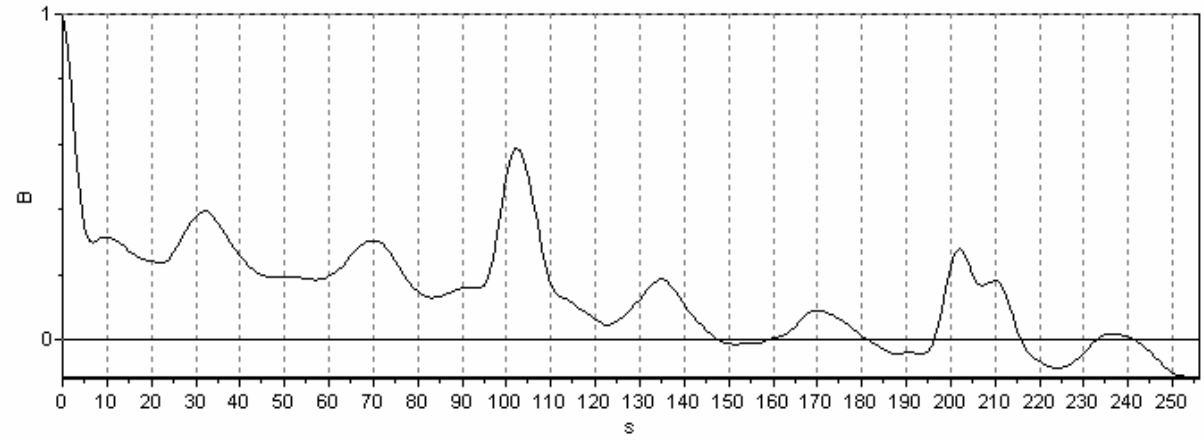

Figure C.8. Autocorrelation Function Graphic of Person-1 & State-4 (Application-2)